



#### RESEARCH ARTICLE

10.1029/2020PA004110

#### **Key Points:**

- Establishes new method for evaluating preservation quality of benthic foraminifera commonly used to construct geochemical proxy records
- Links Cibicidoides and Uvigerina assemblage preservation at various sites to changes in water mass corrosivity through time
- Quantifies potential diagenetic bias in published stable isotope records and provides guidance on how to avoid such bias in future records

#### **Supporting Information:**

Supporting Information may be found in the online version of this article.

#### Correspondence to:

R. K. Poirier, rpoirier@usgs.gov

#### Citation:

Poirier, R. K., Gaetano, M. Q., Acevedo, K., Schaller, M. F., Raymo, M. E., & Kozdon, R. (2021). Quantifying diagenesis, contributing factors, and resulting isotopic bias in benthic foraminifera using the Foraminiferal Preservation Index: Implications for geochemical proxy records. *Paleoceanography and Paleoclimatology*, 36, e2020PA004110. https://doi.org/10.1029/2020PA004110

Received 4 SEP 2020 Accepted 14 APR 2021

@ 2021. American Geophysical Union. All Rights Reserved.

# Quantifying Diagenesis, Contributing Factors, and Resulting Isotopic Bias in Benthic Foraminifera Using the Foraminiferal Preservation Index: Implications for Geochemical Proxy Records

Robert K. Poirier<sup>1,2</sup>, Madison Q. Gaetano<sup>3,4</sup>, Kimberly Acevedo<sup>5,6</sup>, Morgan F. Schaller<sup>7</sup>, Maureen E. Raymo<sup>1</sup>, and Reinhard Kozdon<sup>1</sup>

<sup>1</sup>Division of Biology and Paleo-Environment, Lamont-Doherty Earth Observatory of Columbia University, Palisades, NY, USA, <sup>2</sup>Now at Florence Bascom Geoscience Center, U.S. Geological Survey, Reston, VA, USA, <sup>3</sup>Department of Geology, College of William and Mary, Williamsburg, VA, USA, <sup>4</sup>Now at Department of Geology, University of Cincinnati, Cincinnati, OH, USA, <sup>5</sup>Division of Biology, Dominican College of Blauvelt, Orangeburg, NY, USA, <sup>6</sup>Now at Organismic and Evolutionary Biology Program, University of Massachusetts Amherst, Amherst, MA, USA, <sup>7</sup>Department of Earth and Environmental Sciences, Rensselaer Polytechnic Institute, Troy, NY, USA

**Abstract** Geochemical records generated from the calcite tests of benthic foraminifera, especially those of the genera Cibicidoides and Uvigerina, provide the basis for proxy reconstructions of past climate. However, the extent to which benthic foraminifera are affected by postdepositional alteration is poorly constrained. Furthermore, how diagenesis may alter the geochemical composition of benthic foraminiferal tests, and thereby biasing a variety of proxy-based climate records, is also poorly constrained. We present the Foraminiferal Preservation Index (FPI) as a new metric to quantify preservation quality based on objective, well-defined criteria. The FPI is used to identify and quantify trends in diagenesis temporally, from late Pliocene to modern coretop samples (3.3-0 Ma), as well as spatially in the deep ocean. The FPI identifies the chemical composition of deep-ocean water masses to be the primary driver of diagenesis through time, while also serving as a supplementary method of identifying periods of changing water mass influence at a given site. Additionally, we present stable isotope data ( $\delta^{18}$ O,  $\delta^{13}$ C) generated from individual Cibicidoides specimens of various preservation quality that demonstrate the likelihood of significant biasing in a variety of geochemical proxy records, especially those used to reconstruct past changes in ice volume and sea level. These single-test data further demonstrate that when incorporating carefully selected tests of only the highest preservation quality, robust paleorecords can be generated.

#### 1. Introduction

Over the last 65 years, the most widely applied proxies to reconstruct paleoclimate records through time are generated from the calcium carbonate (calcite) shells (tests) of foraminifera. Many benthic taxa have far-reaching geographical distributions throughout the deep ocean and feature one of the most complete fossil records of any group of organisms in Earth's history. Pioneering studies demonstrated that these organisms secrete their calcite tests near chemical-equilibrium with seawater, with generally established offsets (e.g., Emiliani, 1955; N. Shackleton, 1967; N. J. Shackleton & Hall, 1984; N. J. Shackleton et al., 1984). Despite the extensive generation of proxy records using benthic foraminifera, especially those relevant to reconstructing past ice volume and sea level (e.g., Ahn et al., 2017; Billups & Schrag, 2002; Elderfield et al., 2010, 2012; Ford et al., 2016; Imbrie et al., 1984; Lear et al., 2000; Lisiecki, 2014; Lisiecki & Raymo, 2005; Raymo et al., 1989; Rosenthal et al., 1997; Ruddiman et al., 1989; S. Sosdian & Rosenthal, 2009; Waelbroeck et al., 2002), the extent to which postdepositional diagenesis might bias the geochemical composition of their tests is still poorly constrained (e.g., Raymo et al., 2018).

While the influence of diagenesis on planktic foraminifera has recently received increasing attention, only a few critical studies have assessed the susceptibility of benthic foraminifera to diagenetic alteration and potential effects on the veracity of proxy records (e.g., Detlef et al., 2020; Edgar et al., 2013; Hasenfratz et al., 2017; Leutert et al., 2019; McCorkle et al., 1995; Millo et al., 2005; Raymo et al., 2018; Sexton &

POIRIER ET AL. 1 of 32



10.1029/2020PA004110

Wilson, 2009). This is due to several assumptions about the robustness of benthic tests relative to those of planktic foraminifera. Tests of benthic taxa are generally less porous and more thickly calcified and are therefore thought to be less susceptible to alteration. Furthermore, as diagenesis likely starts in an environment near the sediment—water interface, any alteration that may occur is thought to reflect relatively similar conditions to those at the sea floor where benthic foraminifera secreted their tests (e.g., Fantle et al., 2010; Pearson & Burgess, 2008; Rudnicki et al., 2001). However, there is increasing evidence that upward diffusion of pore fluids may interact with buried foraminifera even in relatively young deep-sea sediments (e.g., Wycech et al., 2016).

To quantify the extent to which diagenesis affects deep-sea benthic foraminifera, and to identify the most important contributing factors leading to diagenetic alteration, we have developed a new metric called the Foraminiferal Preservation Index (FPI). This metric establishes objective criteria to determine how well an individual test is preserved, while facilitating the quantification of trends in whole assemblage preservation both temporally and spatially. We identify regional trends in FPI assemblage data that are linked to changes in water mass chemistry on glacial–interglacial time scales from the late Pliocene to the modern Holocene (i.e., 3.3–0 million years ago [Ma]). As to avoid confusion with the existing literature, our late Pliocene sampling interval includes the period from  $\sim 3.3$  to 2.9 Ma referred to previously as the mid-Pliocene Warm Period (e.g., Dowsett et al., 2019; Raymo et al., 2018). Finally, we quantify the extent to which the inclusion of even a single slightly altered test in pooled geochemical analyses may bias climatic signals in proxy reconstructions. Overall, this work emphasizes the need to carefully select only the best-preserved benthic foraminifera tests for such analyses in order to generate the most robust climate records.

#### 2. Benthic Foraminifera and Preservation

Over the last century, foraminifera have been the primary source for geochemical data used to construct the majority of long-term climate records. Specifically, benthic species of *Cibicidoides* (including the genus now referred to as *Cibicides*) and *Uvigerina* are commonly used to generate geochemical proxy records from the deep sea due to their relative abundance and geographical/bathyal distributions in the global ocean. Furthermore, the  $\delta^{18}$ O in tests of these taxa is well calibrated with temperature and ambient sea water  $\delta^{18}$ O ( $\delta^{18}$ O<sub>sw</sub>) in addition to the  $\delta^{13}$ C of *Cibicidoides* specimens being useful to compare with different water masses (e.g., N. J. Shackleton & Hall, 1984; N. J. Shackleton et al., 1995). As such, stable isotope ( $\delta^{18}$ O,  $\delta^{13}$ C) and trace metal proxy records (Mg/Ca, Sr/Ca, etc.), among others, generated from these taxa are used to reconstruct changes in deep-sea temperature, ice volume, and deep-ocean circulation through time.

While these taxa are generally assumed to be impervious to diagenesis, or at worst only minimally susceptible to diagenetic alteration, very little work has been done to explore these assumptions until recently (e.g., Detlef et al., 2020; Edgar et al., 2013; Fantle et al., 2010; Leutert et al., 2019; Pearson & Burgess, 2008; Raymo et al., 2018; Rudnicki et al., 2001; Sexton & Wilson, 2009; Sexton et al., 2006). Previous definitions used to identify well-preserved tests suitable for analysis relative to those less well preserved are vague and highly subjective. For example, the term "glassy" has been used to describe well-preserved tests, whereas "frosty" refers to moderately to poorly preserved tests (e.g., Sexton et al., 2006). However, some workers might identify a glassy test as being completely transparent, while others might accept a partially transparent to translucent test as also being well preserved. Furthermore, interpretation of "frosty" tests likely varies among various workers from being translucent to opaque, in addition to possibly being interpreted differently from a test having a shiny versus matte luster or surface texture. The subjective nature of choosing which tests are well preserved and therefore suitable for geochemical analysis is compounded by the fact that in many lab groups, this work is often done by students whom may not have had formal training regarding preservation quality. Herein, we separate Cibicidoides and Uvigerina specimens into three categories representing various states of preservation quality and provide clear definitions of how to identify each in any given sample from any given site (Figures 1-3; Plates S1-S6 in the Supporting Information). Ultimately, we provide visual and geochemical evidence to support these classifications representing various stages of diagenetic alteration and discuss the processes driving the majority of alteration below.

POIRIER ET AL. 2 of 32

25724525, 2021, 5, Downloaded from https://agupubs.onlinelibrary.wiley.com/doi/10.1029/2020PA004110, Wiley Online Library on [18/09/2023]. See the Terms

-and-conditions) on Wiley Online Library for rules of use; OA articles are governed by the applicable Creative C

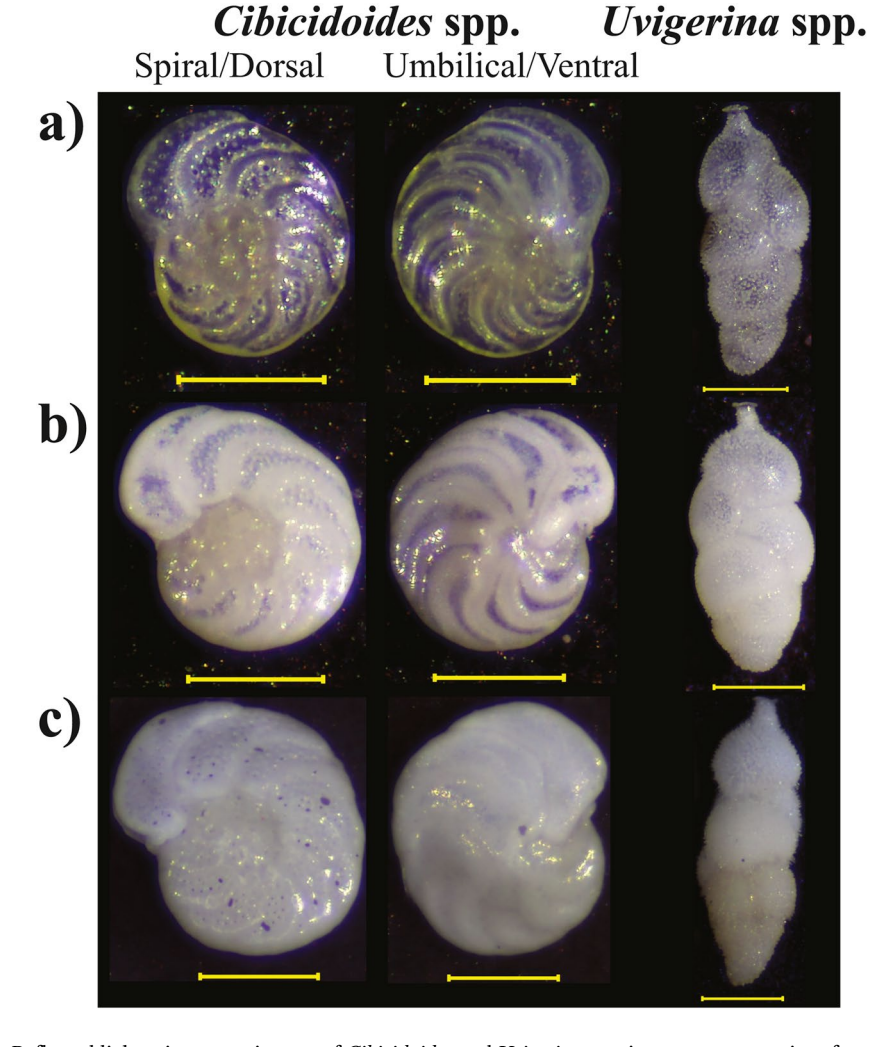


**Figure 1.** Reflected light microscope images of *Cibicidoides* and *Uvigerina* specimens representative of our three defined preservation states: (a) glassy, (b) pseudo-glassy, and (c) frosty. Yellow scale bars represent 250 µm.

#### 2.1. Preservation States Based on Visible Light Microscopy

#### 2.1.1. Glassy Preservation

While we still refer to well-preserved *Cibicidoides* and *Uvigerina* specimens as "glassy," we provide new criteria for this preservation classification. Well-preserved glassy *Cibicidoides* specimens range from being translucent to completely transparent, sometimes with a yellowish-brownish hue. When present, this hue is typically observed within sutures, the umbilicus, and/or along the periphery of the test. Glassy tests are best identified with binocular microscopes by the appearance of their sutures. Sutures in dry glassy tests exhibit no whitening and appear as dark, transparent bands when using reflected light and a black background such as that of a micropaleontological slide or picking tray (Figure 1a; Plate S1 in the Supporting Information). In benthic foraminifera with bilamellar chamber wall construction, including *Cibicidoides*, sutures separate individual chambers that are added incrementally as the organism grows (e.g., Gupta, 1999). Whereas a new layer of calcite is secreted over the exterior of each chamber when a new chamber is formed, sutures represent a single generation of calcite. This may explain why sutures tend to exhibit the first stages of visible "whitening" when viewing altered tests under a binocular microscope. *Cibicidoides* specimens also can contain randomly distributed particles (fine sedimentary grains, e.g., quartz) that are not secreted by the organism and may either be agglutinated or represent contaminations within the organic layer separating different layers of calcite (e.g., Gupta, 1999). These inclusions may be related to the yellowish-brownish hue

POIRIER ET AL. 3 of 32

sometimes exhibited in glassy tests or could possibly correspond with the visible whitening associated with increased porosity apparent in cross section via scanning electron microscopy (SEM) imaging of altered tests (Section 2.2). For our quantitative classification scoring scheme outlined below, we define a *Cibicidoides* specimen as glassy with the vast majority of its chambers being transparent and little to no whitening of the sutures. Therefore, a test with slight whitening of one or two chambers (often the final chamber) may still be considered glassy.

Glassy *Uvigerina* specimens largely exhibit the same features of glassy *Cibicidoides* specimens, with a few caveats. Similar to *Cibicidoides*, *Uvigerina* taxa also exhibit bilamellar chamber wall construction (e.g., Gupta, 1999). Ideally preserved *Uvigerina* are translucent to completely transparent in the majority of their chambers, with very distinct and defined test ornamentation (Figure 1a; Plate S4 in the Supporting Information). Depending on the species, test ornamentation may make it challenging to distinguish a glassy *Uvigerina* specimen with thickly calcified ornamentation from a comparable, yet altered test (Sections 2.1.2 and 2.1.3). In such cases, it is often possible to apply the same transparent versus translucent assessment of the ornamentation itself to classify the preservation. For example, if the majority of the chamber ornamentation of a dry *Uvigerina* specimen appears primarily transparent under a binocular microscope the test is considered to be glassy. Alternatively, if the ornamentation appears translucent to opaque throughout the majority of the surface area, the test is not considered to be glassy.

#### 2.1.2. Pseudo-Glassy Preservation

Our newly defined "pseudo-glassy" preservation state represents tests that fall in-between the traditional "glassy" (Section 2.1.1) versus "frosty" (Section 2.1.3) designations, which we refine herein. *Cibicidoides* and *Uvigerina* specimens exhibiting pseudo-glassy preservation have chambers that are primarily translucent to transparent (early chambers in *Uvigerina* specimens can also appear slightly opaque), with whitened sutures and/or whitening of few to several (i.e., not all) chambers (Figure 1b; Plates S2 and S5 in the Supporting Information). As discussed above, it can be difficult to distinguish whether a *Uvigerina* specimen is of glassy or pseudo-glassy preservation due to thick test ornamentation. A *Uvigerina* specimen is considered pseudo-glassy when the majority of its test ornamentation appears translucent to opaque.

Importantly, if a pseudo-glassy *Cibicidoides* or *Uvigerina* specimen becomes wet, it will likely resemble a glassy test. It is imperative that the preservation determination occurs when tests are completely dry. As many of the tests we consider to be of this pseudo-glassy preservation state can closely resemble glassy tests with slightly whitened sutures, particularly in *Cibicidoides* specimens, it is certainly possible that pseudo-glassy tests could have been selected for geochemical analysis in many previous studies. The potential inclusion of these types of tests in geochemical analyses is critically explored below to determine to what extent such tests could bias proxy records (Sections 4.4–5).

#### 2.1.3. Frosty Preservation

Our classification of "frosty" *Cibicidoides* and *Uvigerina* specimens is defined by most of the test exhibiting substantial whitening, with the vast majority of chambers being opaque (Figure 1c; Plates S3 and S6 in the Supporting Information). In many "frosty" *Uvigerina* specimens, the youngest one or two chambers may still be translucent to transparent, while the rest of the test is completely whitened and opaque. While this generally aligns with the traditional definition for frosty tests, we identify the opaqueness of the chambers to be the most important indicator of substantial diagenetic alteration relative to the surface luster (i.e., shiny vs. matte in appearance). However, we consider a shiny surface luster to indicate a relatively less altered test than one with a matte surface luster (Section 2.2). Finally, we note that surface ornamentation on some "frosty" *Uvigerina* specimens sometimes appears to have secondary inorganic calcite overgrowths (e.g., specimens v and vi in Figure 3) similar to those noted on frosty planktic foraminifera (e.g., Raymo et al., 2018; Sexton et al., 2006).

#### 2.2. Scanning Electron Microscopy: Cross-Section Imaging by Preservation State

To explore the cause of visible whitening of sutures and chambers in diagenetically altered *Cibicidoides* and *Uvigerina* specimens, we examined the internal wall structure of tests from each preservation state (Figures 2 and 3). This was accomplished by mounting glassy, pseudo-glassy, and frosty specimens of each

POIRIER ET AL. 4 of 32

2572425, 2021, 5, Downloaded from https://agupub.sonlinelibarry.wiley.com/doi/10.1029/2020PA004110, Wiley Online Library on [18/09/203]. See the Terms and Conditions (https://onlinelibarry.wiley.com/terms-and-conditions) on Wiley Online Library for rules of use; OA articles are governed by the applicable Creative Commons Licens

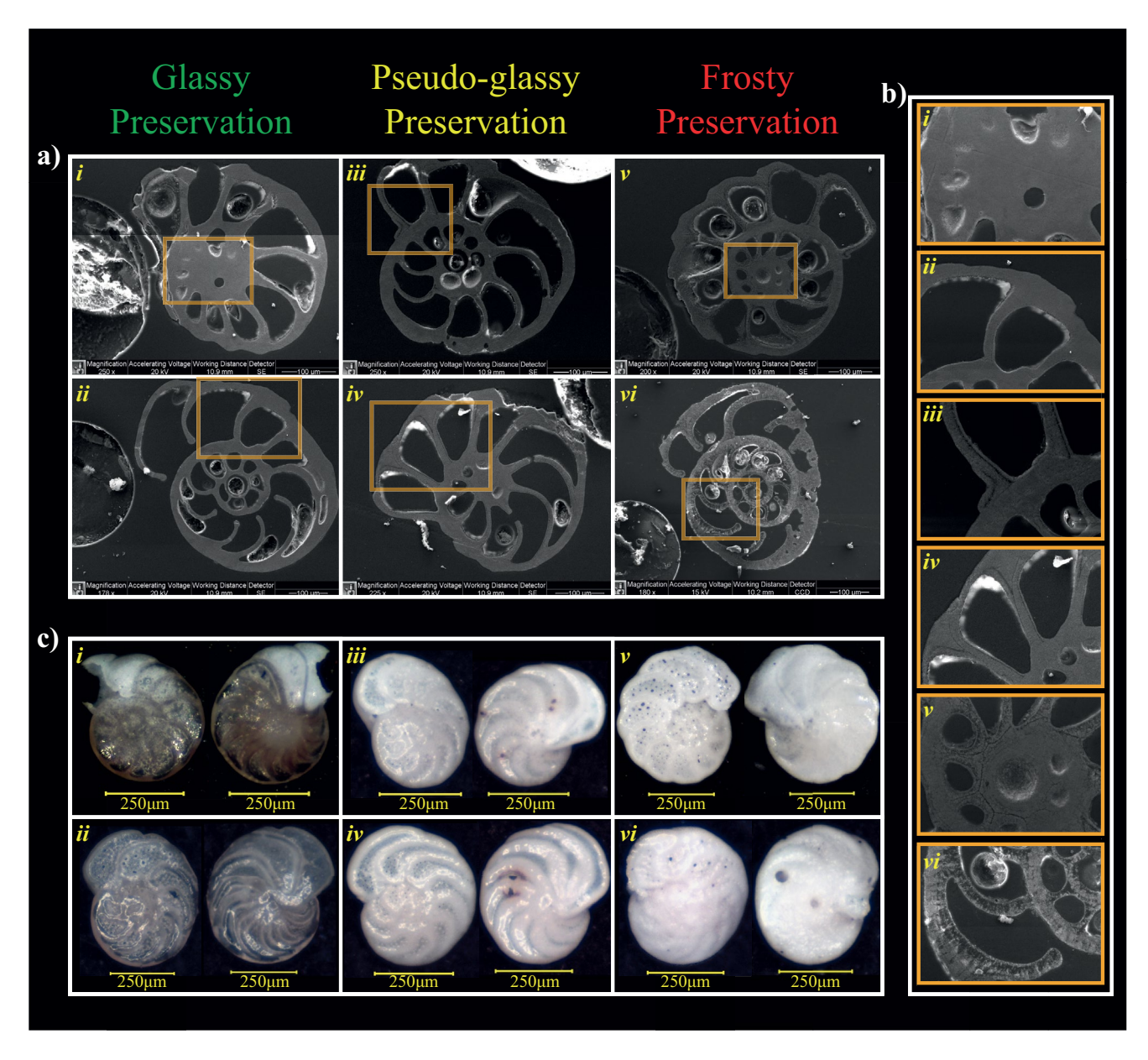


Figure 2. (a) Scanning electron microscopy (SEM) images (magnifications varying from 178X to 250X) of six *Cibicidoides* specimens, including two of each preservation state defined by this study. Outlined midsection regions in (a) are magnified in (b), demonstrating the integrity of internal chamber wall structure in each preservation state. Reflected light images of each corresponding test are shown in (c).

genus in epoxy mounts, which were then ground and polished to midsection. Mounted tests were then imaged in high resolution using the FEI/Philips XL30 scanning electron microscope (SEM) at the Imaging and Analysis Center of Princeton University.

When examining the cross-section SEM images, several observations are apparent and consistent for the various preservation states of *Cibicidoides* and *Uvigerina* specimens (Figures 2 and 3). First, ideal glassy tests demonstrate densely calcified, microgranular chamber walls and sutures throughout the entire test cross sections, which appear visibly smooth and homogeneous, with little to no visible evidence of growth bands. Second, pseudo-glassy tests demonstrate pronounced dark bands running parallel to calcite layers of individual chambers, likely representing domains previously occupied by organic membrane growth layers and are now essentially void spaces. Additionally, the calcite in most pseudo-glassy tests appears to be less homogeneous and more granular relative to glassy tests. Finally, the trends observed in pseudo-glassy tests

POIRIER ET AL. 5 of 32

2572425, 2021, 5, Downloaded from https://agupubs.onlinelibary.viley.com/doi/10.1029/2020PA004110, Wiley Online Library on [18/092023]. See the Terms and Conditions (https://onlinelibrary.wiley.com/terms-and-conditions) on Wiley Online Library for rules of use; OA articles are governed by the applicable Creative Communications (https://onlinelibrary.wiley.com/terms-and-conditions) on Wiley Online Library for rules of use; OA articles are governed by the applicable Creative Communications (https://onlinelibrary.wiley.com/terms-and-conditions) on Wiley Online Library for rules of use; OA articles are governed by the applicable Creative Communications (https://onlinelibrary.wiley.com/terms-and-conditions) on Wiley Online Library for rules of use; OA articles are governed by the applicable Creative Communications (https://onlinelibrary.wiley.com/terms-and-conditions) on Wiley Online Library for rules of use; OA articles are governed by the applicable Creative Communications (https://onlinelibrary.wiley.com/terms-and-conditions) on Wiley Online Library for rules of use; OA articles are governed by the applicable Creative Communications (https://onlinelibrary.wiley.com/terms-and-conditions) on Wiley Online Library for rules of use; OA articles are governed by the applicable Creative Communications (https://onlinelibrary.wiley.com/terms-and-conditions) on Wiley Online Library for rules of use; OA articles are governed by the applicable Creative Communications (https://onlinelibrary.wiley.com/terms-and-conditions) on Wiley Online Library for rules of use; OA articles are governed by the applicable Creative Communications (https://onlinelibrary.wiley.com/terms-and-conditions) on Wiley Online Library for rules of use; OA articles are governed by the applicable Creative Communications (https://onlinelibrary.wiley.com/terms-and-conditions) on Wiley Online Library for rules of use; OA articles are governed by the applicable Creative Communications (https://onlinelibrary.wiley.com/terms-and-conditions) on Wiley Online Librar

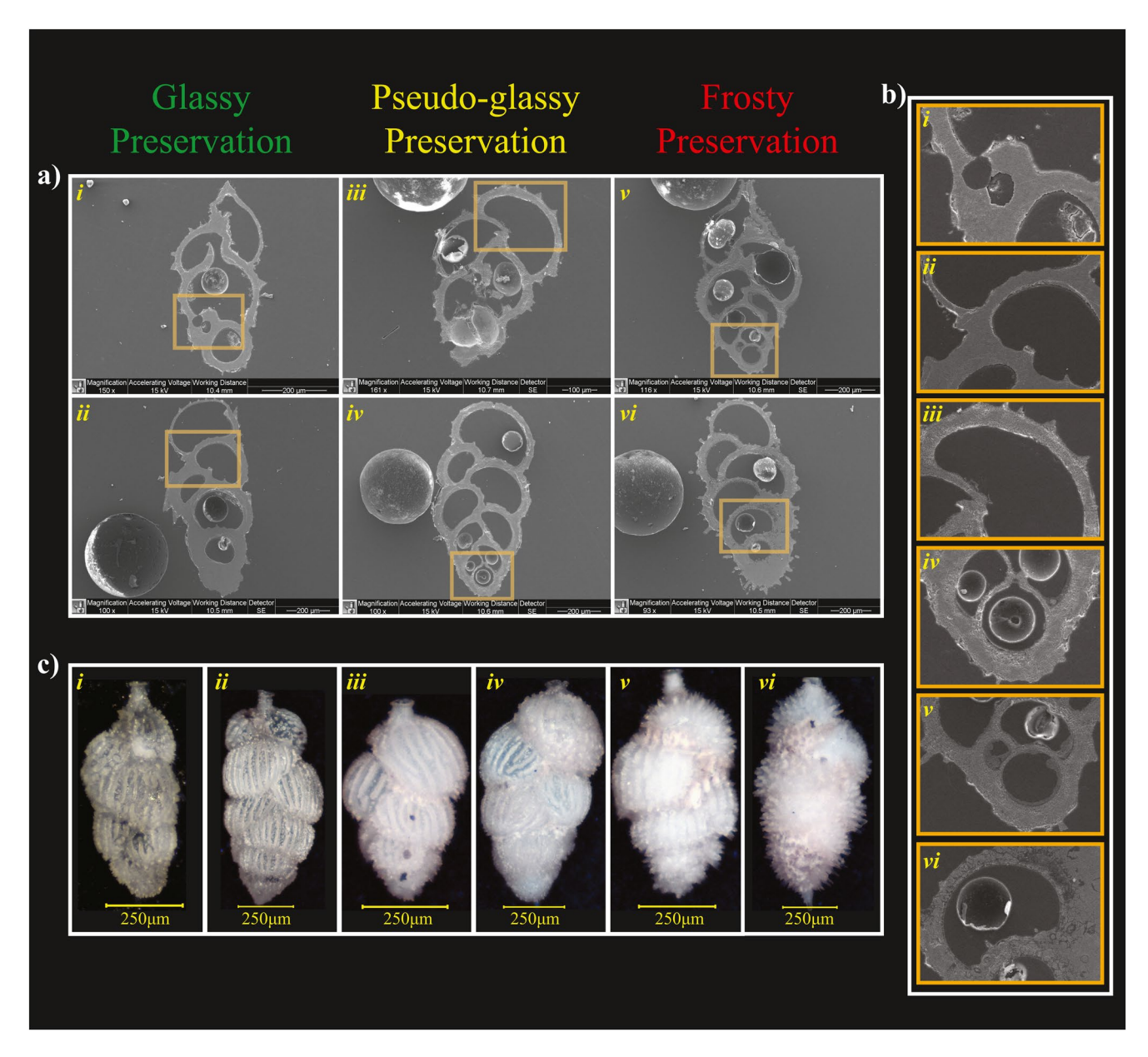


**Figure 3.** (a) Scanning electron microscopy (SEM) images (magnifications varying from 63X to 161X) of six *Uvigerina* specimens, including two of each preservation state defined by this study. Outlined midsection regions in (a) are magnified in (b), demonstrating the integrity of internal chamber wall structure in each preservation state. Reflected light images of each corresponding test are shown in (c).

appear even more pronounced within those of frosty preservation. Enlarged growth bands are very apparent in frosty tests, likely from decomposed organic membrane layers, and are associated with widespread dark void space through much of the material, especially within the inner chamber walls (Figures 2a and 2b:  $\nu$  and  $\nu i$ ). While this is the first study to document these features related to diagenetic alteration in *Cibicidoides* and *Uvigerina* specimens, others made similar observations in different benthic genera (e.g., Detlef et al., 2020).

Based on these apparent trends visible in high-resolution SEM cross-section images, we propose that diagenetic alteration likely begins early after deposition. This is supported by tests of each preservation state often being present within any given sample ranging from modern coretops to samples that are millions of years old (Plates S1–S53 in the Supporting Information). Such alteration appears related to the initial decompo-

POIRIER ET AL. 6 of 32

2572425, 2021, 5, Downloaded from https://agupubs.onlinelibrary.wiley.com/doi/10.1029/2020PA004110, Wiley Online Library on [18/09/2023]. See the Terms and Conditions (https://onlinelibrary.wiley.com/terms-and-conditions) on Wiley Online Library for rules of use; OA articles are governed by the applicable Cerative Commons. License

Pliocene References Note. References: (1) Mayer et al. (1992), (2) Curry et al. (1995), (3) Harris et al. (1997), (4) Keigwin et al. (1998), (5) Gersonde et al. (1999), (6) Wang et al. (2000), (7) Hodell et al. (2001), (8) 0.0 - 0.40.0 - 0.80.1 - 0.40.1 - 1.10.1 - 1.1N/A Organic carbon content (wt. %) Pleistocene 0.1-1.10.0 - 0.80.1 - 0.40.1-1.10.0 - 0.4N/A Pleistocene Holocene 0.0 - 0.8to mid-0.0-0.4 0.3 - 0.70.3 - 1.60.1-1.10.1-1.1N/APliocene 10-40 09-0 10-80 0-75  $\sim 50$ Carbonate content (wt. %) Pleistocene 10-40 09-0 Pleistocene Holocene to mid-10-40 10 - 3010-80 09-0 0-75 Pliocene 2.0 - 4.08.1 - 8.23.6 - 4.5N/A2.4 Sedimentation rates (cm/kyr) Pleistocene 2.0-4.0 8.1-8.2 3.6-4.5 8.5 - 11.03.3 - 5.02.5 - 3.3~4.0 Pleistocene Holocene 12.8-15.0 to mid-2.5 - 3.32.0 - 4.04.9 - 6.2Site Information and Sediment Characteristics Water depth 4,620 4,356 2,772 3,346 3,052 2,997 Œ Longitude -43.7409.894 113.285 -90.818-75.419158.202 (°E) Latitude 5.976 31.674 -3.095-40.93636.127  $\tilde{\mathbf{z}}$ ODP

Bralower et al. (2002), (9) Grützner e al. (2002), and (10) Sexton & Barker (2012). 'Site only studied for the last deglaciation. sition of the organic membrane associated with growth bands within the chamber wall. We hypothesize that the microbial decomposition of the organic membrane may either cause a corrosive microenvironment, which then leads to continued dissolution of wall material progressively over time, or that the decomposition of the organic membrane results in void space that is then accessible for porewater intrusion leading to progressive diagenetic alteration (e.g., Johnstone et al., 2010).

Ultimately, the degree of diagenetic alteration distinguishes our three preservation states. Individual tests within any given assemblage that remain glassy through time are seemingly protected by advantageous microenvironmental conditions, possibly including localized pockets of densely consolidated clay/silt sized particles, likely devoid of significant amounts of organic material and thereby inhibiting microbial decomposition (e.g., Pearson & Burgess, 2008; Sexton & Wilson, 2009). Overall, it is apparent that the visible whitening of sutures and chambers, resulting in tests eventually becoming opaque, is driven primarily by dissolution. Such calcite dissolution in benthic foraminifera can also be accompanied by secondary recrystallization (Detlef et al., 2020). Therefore, both of these processes likely contribute not only to the change in visible preservation, but also the geochemical composition of the entire test (Section 4.4).

#### 3. Materials and Methods

#### 3.1. Study Sites and Hydrography

In addition to providing clear and succinct definitions and visual references to aid in the identification of various stages of diagenetic alteration in tests of the benthic genera *Cibicidoides* and *Uvigerina*, this study sought to determine what processes and/or conditions might drive such diagenesis and quantify the extent to which it might bias  $\delta^{18}$ O and  $\delta^{13}$ C proxy records. To accomplish these goals, we studied samples from seven deep-sea sediment cores (Table 1 and Figure 4). Sediments from these cores recovered by the International Ocean Discovery Program (IODP) and its predecessor programs sample the entire range in deep-ocean water mass chemistry as well as the typical range of sedimentation rates and physical sediment characteristics found in most deep-sea regions that produce the majority of proxy records (Table 1).

#### 3.1.1. Atlantic Sites

Sediment samples recovered from the deep Atlantic Ocean sites are bathed by water masses representing end-member chemical properties within the Atlantic meridional overturning circulation (AMOC) system. These include northern component waters, referred to here as North Atlantic Deep Water (NADW), and southern component waters, referred to here as Antarctic Bottom Water (AABW). North Atlantic Sites 925 and 1059, located on the Ceara Rise and the Blake Outer Ridge, respectively, are presently bathed by waters in the core of NADW (Table 1 and Figure 4). During glacial periods, these sites were likely still influenced by NADW, widely referred to as glacial North Atlantic Intermediate Water (GNAIW), although to a lesser degree as it shoaled to shallower depths. Recent studies sometimes refer to this glacial water mass reflecting decreased percentages of NADW with increased AABW and subtropical water components (e.g., Gebbie, 2014; Oppo et al., 2018) as glacial North Atlantic Deep Water (GNADW) (e.g., Howe et al., 2016). Importantly, the proxy and model compilations of Oppo et al. (2018) demonstrate higher proportions of GNAIW/GNADW in the region near Site 925, with a higher subtropical component, relative to similar depths near Site 1059 where a higher proportion of AABW was likely present during the Last Glacial Maximum.

POIRIER ET AL. 7 of 32

25724525, 2021, 5, Downloaded from https://agupubs.onlinelibarry.wiley.com/doi/10.1029/2020PA004110, Wiley Online Library on [18/09/2023]. See the Terms and Conditions (https://onlinelibarry.wiley.com/terms-and-conditions) on Wiley Online Library for rules of use; OA articles are governed by the applicable Creative Commons Licenses

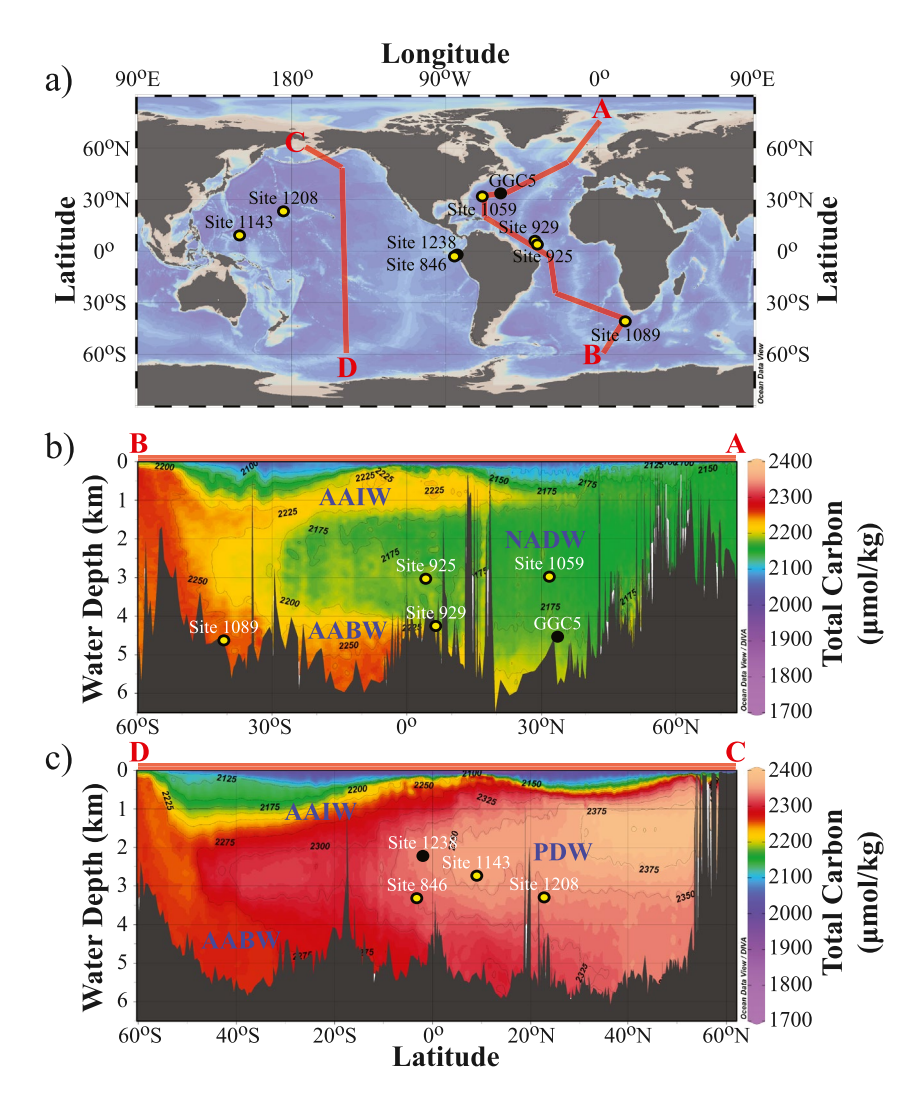


**Figure 4.** Map (a) and cross sections of the distribution of our study sites in the (b) deep Atlantic Ocean and (c) the deep Pacific Ocean, identifying the location of sites used in this study (yellow dots). Black dots indicate the location of two sites used for comparison to our stable isotope records. Maps and cross sections in this figure were generated using Ocean Data View 5 (Schlitzer, 2020) and the DIVA gridding interpolation tool (Troupin et al., 2012) to visualize total dissolved carbon measured from depth-sampling stations included within the Global Data Analysis Project (GLODAP) v2 data set (Olsen et al., 2016).

The deep South Atlantic Site 1089, on the Agulhas Ridge (Table 1 and Figure 4), is primarily bathed by AABW during both glacial and interglacial periods (Gersonde et al., 1999; Hodell et al., 2001, 2003; Lisiecki, 2014; Oppo et al., 2018; Poirier & Billups, 2014). However, there is discussion as to whether the component of AABW influencing the deep Southern Ocean may be more isolated from that influencing the deep South Atlantic Ocean during glacial periods (e.g., Allen et al., 2015; Oppo et al., 2018; Ronge et al., 2016; Sikes et al., 2017; Ullermann et al., 2016). The proposed explanation for this isolation is discussed as being the result of changing surface hydrography and a corresponding shift in deepwater formation zones during glacial periods.

Finally, the sediment core recovered from deep equatorial North Atlantic Site 929 on the Ceara Rise resides near the present-day mixing boundary between NADW and AABW (Table 1 and Figure 4). As such, this site is particularly sensitive to changes in the distribution of these two water masses over glacial–interglacial cycles (Bickert et al., 1997; Curry et al., 1995; Poirier & Billups, 2014). Generally, the site is primarily influenced by NADW during interglacial periods and by AABW during glacial periods.

POIRIER ET AL. 8 of 32

#### 3.1.2. Pacific Sites

Sites 846 (Carnegie Ridge), 1143 (South China Sea), and 1208 (Shatsky Rise) are all bathed by Pacific Deep Water (PDW), while located in a wide geographic range within the deep Pacific basin (Table 1 and Figure 4). PDW represents some of the oldest and presumably the most corrosive deep water in the modern global deep ocean due to the highest total dissolved carbon content (Figure 4). This high total carbon content is the result of AABW aging as it recirculates throughout the deep Pacific basin without being further ventilated. During glacial periods, a younger and less corrosive water mass is thought to have been present above depths of  $\sim$ 2–3 km in the western Pacific basin, likely with source waters originating in the North Pacific and referred to as glacial North Pacific Intermediate Water (GNPIW), which could potentially include some component of recirculated GNAIW (e.g., Herguera et al., 2010; L. D. Keigwin, 1998; Matsumoto et al., 2002; Okazaki et al., 2010).

Overall, our site selection includes sediment cores with a broad range of characteristics. These include composition, lithology, and sedimentation accumulation rates (Table 1), while sampling the full range of deepwater mass chemical compositions (Figure 4). Within the framework of this study, we aim to quantify geographic and temporal trends in overall assemblage preservation. Such trends should help isolate which factors are most likely to determine the extent to which benthic foraminifera tests are proportionally better or worse preserved through time.

#### 3.2. Sample Selection and Processing

We processed and analyzed a total of 494 sediment samples (Site 846, n=55; Site 925, n=43; Site 929, n=61; Site 1059, n=53; Site 1089, n=82; Site 1143, n=89; and Site 1208, n=111). These include samples from peak interglacial and glacial periods throughout the late Pliocene to the modern Holocene (3.3–0 Ma) from Sites 846, 925, 929, 1089, 1143, and 1208, as well as samples spanning the last deglaciation from Sites 846, 929, 1059, and 1089. The sampling intervals for each core were chosen based on published stable isotope records (i.e., Bickert et al., 1997; Billups et al., 1998; Cheng et al., 2004; deMenocal et al., 1997; Franz & Tiedemann, 2002; Hagen & Keigwin, 2002; Hess & Kuhnt, 2005; Hodell et al., 2001; Mix et al., 1995; N. J. Shackleton et al., 1995; Venti & Billups, 2012; Wilkens et al., 2017) and corresponding age models tuned to deep-sea benthic  $\delta^{18}$ O stacks (i.e., Ahn et al., 2017; Lisiecki & Raymo, 2005). Many of these interglacial and glacial periods are of particular interest to researchers applying foraminiferal geochemistry to the evolution of orbital-scale climate cycles, changes in ice volume and sea level, and deep-sea  $CO_2$  storage.

All sediment samples selected for this study were processed following standard procedures. After freeze-drying for 48 h, sediment samples were weighed (average mass of 15.8 g, range of 2.9–34.9 g), washed through a 63- $\mu$ m sieve, and oven dried at 50°C for 24 h. From each >63- $\mu$ m sediment sample, all specimens of the genera *Cibicidoides* and *Uvigerina* were picked from the 150–250  $\mu$ m and >250  $\mu$ m size fractions. Using a binocular microscope, each individual *Cibicidoides* and *Uvigerina* specimen was critically evaluated for preservation quality allowing us to quantify the whole assemblage preservation of each genera from each sample (Section 3.3). Finally, from samples spanning the last deglaciation featuring high abundances of *Cibicidoides*, specimens of varying preservation quality were chosen for single-test stable isotope analyses (Section 3.4).

#### 3.3. The Foraminiferal Preservation Index

To quantify preservation quality and changes through time in *Cibicidoides* and *Uvigerina* assemblages, we developed the FPI. To generate an assemblage preservation score using the FPI, each individual test must first be assigned to one of the three preservation states outlined above (i.e., glassy, pseudo-glassy, or frosty). Next, each test  $\geq 150 \, \mu m$  is assigned a numerical value, referred to here as an initial score (IS) from 3 to 5 (i.e., IS3–IS5<sub>glassy</sub>, IS3–IS5<sub>pseudo-glassy</sub>, and IS3–IS5<sub>frosty</sub>). For a test to receive an IS5 value, it must be an ideal test regardless of preservation state, with very clearly defined whorls, sutures, pores, and other surface features (i.e., aperture and test ornamentation). For example, we assigned IS5 values for *Cibicidoides* specimens in Figures 1a and 1b; the *Uvigerina* specimen in Figure 1a; *Cibicidoides* specimens ii and iv in Figure 2; and *Uvigerina* specimens i-iii, v, and vi in Figure 3. We emphasize that this IS value is assigned solely on the in-

POIRIER ET AL. 9 of 32

tegrity of all surface features. Thus, even a frosty test can receive an IS5 value, although this is less common. A test with an IS3 value usually contains enlarged pores and "smoothed" looking surface features, including sutures and surface ornamentation (e.g., *Cibicidoides* specimen *vi* in Figure 2). In such tests, chambers in early whorls are often difficult to distinguish from one another as a consequence of such "smoothing." An IS4 value is assigned to tests with more subtly smoothed features, and/or slightly enlarged pores, but not to the same degree as a test with an IS3 score (e.g., *Cibicidoides* specimen in Figure 1c; *Uvigerina* specimens in Figures 1b and 1c; *Cibicidoides* specimens *i*, *iii*, and *v* in Figure 2; and *Uvigerina* specimen *iv* in Figure 3).

From the IS3–5 value for a given test, deductions of 1–2 points are applied to generate its final score (FS). A deduction of one point is applied for either a missing or fractured chamber, and/or evidence of slight dissolution. A deduction of two points is applied for extensive missing or fractured chambers, and/or evidence of extensive dissolution. For example, an assigned FS1 value for a test could be the result of highly smoothed surface features, with some combination of extensive dissolution pockmarks and/or one to several fractured/missing chambers (i.e., IS3 – 2 = FS1). Additional visual references of our FS score assignments for *Cibicidoides* and *Uvigerina* specimens are provided in Plates S1–S53 of the Supporting Information. We note that several *Uvigerina* specimens in Plates S4–S6 have three circular laser-ablation holes (i.e., not evidence of dissolution), with data to be published in a subsequent study.

To generate a whole assemblage FPI preservation score, a tally of each FS1–5 valued tests within each preservation state must be recorded (i.e., the total number of tests in each of the following categories: nFS1<sub>glassy</sub>; nFS2<sub>glassy</sub>; nFS2<sub>glassy</sub>; nFS2<sub>glassy</sub>; nFS2<sub>glassy</sub>; nFS3<sub>glassy</sub>; nFS3<sub>glassy</sub>; nFS3<sub>glassy</sub>; nFS3<sub>grosty</sub>; nFS3

$$\left( \left( \sum (\text{nFS1}_{glassy} * 1, \text{nFS2}_{glassy} * 2, \text{nFS3}_{glassy} * 3, \text{nFS4}_{glassy} * 4, \text{nFS5}_{glassy} * 5) * 10 \right) + \\ \left( \sum (\text{nFS1}_{pseudo-glassy} * 1, \text{nFS2}_{pseudo-glassy} * 2, \text{nFS3}_{pseudo-glassy} * 3, \text{nFS4}_{pseudo-glassy} * 4, \text{nFS5}_{pseudo-glassy} * 5) * 3 \right) + \\ \left( \sum (\text{nFS1}_{frosty} * 1, \text{nFS2}_{frosty} * 2, \text{nFS3}_{frosty} * 3, \text{nFS4}_{frosty} * 4, \text{nFS5}_{frosty} * 5) * 1 \right) \right) \\ - \\ n_{TOT}$$

FPI assemblage score.

In this equation,  $n_{TOT}$  is the total number of tests within the complete *Cibicidoides* or *Uvigerina* assemblage. The resulting whole assemblage FPI scores range from 1 to 50, where an assemblage with an FPI score of 1 requires every test to have  $FS1_{frosty}$  values (FPI score of 0 means no *Cibicidoides* or *Uvigerina* specimens were present). Likewise, an assemblage with an FPI score of 50 requires each test in that assemblage to have  $FS5_{glassy}$  values. Generally, FPI preservation scores >15 represent a relatively well-preserved assemblage, which is representative of an approximate 2:1 ratio of glassy and pseudo-glassy tests relative to frosty tests. FPI scores <15 indicate a relatively poorly preserved assemblage, and very poorly preserved assemblages produce FPI scores <10, which usually do not contain many glassy tests suitable for geochemical analysis. When generating time series of whole assemblage FPI scores in this manner, our new metric incorporates changes in the relative proportions of tests representing each preservation state, in addition to documenting changes in the relative "completeness" of tests within each preservation group through time. For use in future studies, we include a blank Excel template with the FPI formula in the Supporting Information associated with this manuscript.

To provide an estimate of subjective variability in this quantitative metric measuring changes in qualitative observations, we conducted a series of comparative assessments. Three of the authors scored 100 *Cibici*-

POIRIER ET AL. 10 of 32



10.1029/2020PA004110

doides tests (>250  $\mu$ m) from 13 assemblages within samples from the three deep Pacific sites. These include the first author and two undergraduate summer REU interns, the latter with no prior micropaleontology experience who had just been taught the FPI scoring procedure. At the conclusion of this comparative assessment, two standard deviations of the average for the final FPI scores for the complete sample data set, including the FS by each author for all 100 tests, was 3.11. Therefore, we estimate a subjective human error associated with the FPI metric of  $\pm 3.1$  FPI assemblage score points. It is important to note that the subjective error would likely increase in well-preserved assemblages and decrease in poorly preserved assemblages as a function of the 10:3:1 weighting ratio from glassy to pseudo-glassy to frosty tests (Equation 1).

#### 3.4. Single-Test Stable Isotope Analyses

Once regional and temporal trends were identified in the FPI data from each peak interglacial and glacial time period (Sections 4.1 and 4.2), we generated higher resolution FPI records since the last deglaciation (from ~25 thousand years ago [ka] to the present) from IODP Sites 846, 929, 1059, and 1089 (Section 4.3). This was done to determine the timing of changes in preservation during deglaciation from the deep Atlantic and Pacific basins. From the same time interval, we then conducted single-test stable isotope ( $\delta^{18}$ O and  $\delta^{13}$ C) analyses on multiple Cibicidoides specimens of each preservation state in samples from Site 846 (n = 147 tests) and Site 929 (n = 173 tests). The aim of these analyses was to quantify the extent to which diagenetic alteration in pseudo-glassy and frosty tests might alter their average stable isotope composition relative to glassy tests found in the same sediment samples, and how such offsets might change through time (Section 4.4). Sites 846 and 929 were chosen for single-test stable isotope analyses because they contain a relatively large number of Cibicidoides specimens of each preservation state for this interval. Whenever possible, we conducted single-test stable isotope analyses on three tests of each preservation state from each sample. We also generated single-test stable isotope analyses on samples from Site 1089 (n = 108 tests), but the scarcity of tests of each preservation state prevents the calculation of robust trends throughout the entire deglacial record. As a proof of concept, we also conducted single-test analyses on 76 tests (n = 35Cibicidoides specimens; n = 41 Uvigerina specimens) from Site 846 samples corresponding with MIS 9 and 10. All deglacial single-test data, including those from Site 1089 and the MIS 9-10 single-test data from Site 846 are available in the Supporting Information and at the PANGAEA data repository.

Each test chosen for stable isotope analysis was imaged on both the dorsal (spiral) and ventral (umbilical) sides using reflected light (combination of LED ring light and gooseneck LED illuminators) with a black background via a 5-MP digital camera attached to a binocular microscope. Subsequently, each test was weighed, and tests featuring narrow mass ranges were selected for individual analytical runs of  $\delta^{18}$ O and  $\delta^{18}$ O which allows for the optimization of instrument tuning. The average mass of the tests analyzed was 29.4  $\mu$ g ( $\pm 18.6$  $[1\sigma]$ ; full range from 5 to 245  $\mu$ g). The tests from samples corresponding with the last deglaciation from Sites 849, 929, and 1089 were analyzed on a Thermo Delta V Kiel IV dual inlet mass spectrometer at the Lamont-Doherty Earth Observatory and were corrected relative to the NBS-19 calcite standard. Average precision on these analyses was better than 0.08% for  $\delta^{18}O$  and better than 0.06% for  $\delta^{13}C$ . The tests from Site 846 samples corresponding with MIS 9 and 10 were analyzed on an Isoprime 100 dual inlet mass spectrometer with carbonate multipreparation system at Rensselaer Polytechnic Institute and were corrected relative to the NBS-19 calcite standard. These analyses produced average precision better than 0.06% for  $\delta^{18}$ O and better than 0.03% for  $\delta^{13}$ C. For reference, and as additional visual aids to identify only the best-preserved *Cibicidoides* specimens for future geochemical analyses, we include the visible light images, single-test FPI scores (FS) by preservation state, test weights, and corrected stable isotope results for each individual test analyzed during the last deglacial interval from Sites 846 and 929 (Plates S7–S53 in the Supporting Information).

#### 4. Results and Discussion

# **4.1.** Quantifying Regional and Temporal Trends in Preservation: The Foraminiferal Preservation Index

To determine the ultimate cause underlying variability in the preservation quality of *Cibicidoides* and *Uvigerina* assemblages through time, we assigned FS values (Section 3.3) to 6,313 *Cibicidoides* and 7,900 *Uvigerina* specimens ( $\geq$ 150  $\mu$ m:  $\sim$ 150–500  $\mu$ m for *Cibicidoides* specimens,  $\sim$ 150–1,000  $\mu$ m for *Uvigerina* specimens).

POIRIER ET AL. 11 of 32



10.1029/2020PA004110

These tests were picked from 494 processed core samples from sections covering peak interglacial and peak glacial periods spanning from the late Pliocene to the Holocene (Section 3.2) from IODP Sites 846, 925, 929, 1089, 1143, and 1208 (Figures 5–7). Individual test FS values were used to calculate FPI *Cibicidoides* and *Uvigerina* assemblage scores from samples covering various peak interglacial and glacial periods since the late Pliocene. Overall, these FPI assemblage scores identify several regional and temporal trends. In addition, it is notable that tests from the smaller  $150-250 \,\mu m$  size fraction were generally better preserved than larger tests in the  $\geq 250 \,\mu m$  size fraction in most assemblages at any given site and any given time period (see data available within the Supporting Information).

# 4.1.1. Interglacial Versus Glacial *Cibicidoides* Assemblage Preservation During the Middle-to-Late Pleistocene (1.0-0 Ma) and From the Late Pliocene to Early Pleistocene (3.4-2.4 Ma)

Several regional and temporal trends in *Cibicidoides* assemblage preservation quality can be observed throughout both the 1.0–0 Ma and 3.4–2.4 Ma timeslices (Figure 5). The FPI scores from the deep Pacific Sites 846, 1143, and 1208 suggest that during the middle-to-late Pleistocene, *Cibicidoides* assemblages from glacial periods are generally better preserved than those from interglacial periods (Figures 5a and 7a). Notably, a water-depth gradient in middle-to-late Pleistocene glacial *Cibicidoides* preservation quality is evident between sites in the deep Pacific. Glacial *Cibicidoides* assemblage FPI scores from Site 1143 (2997 m) are generally higher (average glacial FPI assemblage score of 22.5—Figure 7b) than corresponding glacial *Cibicidoides* assemblage FPI scores from the deeper Sites 846 (3,296 m) and Site 1208 (3,346 m) (average glacial FPI scores of 19.0 and 13.6, respectively—Figure 7b).

The same general trends remain consistent in *Cibicidoides* assemblages from the deep Pacific Sites 1143 and 1208 during the late Pliocene to early Pleistocene, with better *Cibicidoides* assemblage preservation within samples from glacial periods (Figures 5c and 7a). Furthermore, the same relation between water depth and glacial *Cibicidoides* preservation quality persists during these older periods, with average glacial FPI scores of 23.5 and 19.6 for Sites 1143 and 1208, respectively (Figure 7c). While these preservation trends are consistent in the deep Pacific Ocean during both study intervals, it is important to note that FPI preservation scores in glacial and interglacial *Cibicidoides* assemblages generally show a higher degree of variability during the older late Pliocene to early Pleistocene timeslice (Figure 5c).

Trends in *Cibicidoides* preservation quality are more variable in the deep Atlantic Ocean, both as a function of latitude and water depth. Similar to documented trends in carbonate accumulation (Hodell et al., 2001, 2003; Sexton & Barker, 2012), *Cibicidoides* assemblage preservation quality in middle-to-late Pleistocene samples from the deep South Atlantic Site 1089 (4,620 m) is comparable to those from sites in the deep Pacific Ocean, with generally higher FPI scores during glacial periods (Figures 5b and 7a). Specifically, the average glacial *Cibicidoides* assemblage FPI score of 18.3 from the South Atlantic Site 1089 samples is comparable to that of Pacific Site 846, while lower than that from samples of Pacific Site 1143 and higher than that of Pacific Site 1208 (Figure 7b). Comparatively, middle-to-late Pleistocene interglacial *Cibicidoides* assemblages in samples from Site 1089 were typically very poorly preserved with lower average FPI scores (5.5) relative to corresponding assemblages in samples from the deep Pacific Sites 846 (FPI = 14.0), 1143 (FPI = 11.6), and 1208 (FPI = 8.1) (Figure 7b).

Inverse to the trends observed in samples from sites in the deep South Atlantic and the deep Pacific, interglacial *Cibicidoides* assemblages in samples from the deep North Atlantic Sites 925 and 929 during the middle-to-late Pleistocene were generally better preserved than glacial assemblages (Figures 5b and 7a). Interglacial *Cibicidoides* assemblages in samples from the deeper North Atlantic Site 929 (4,356 m) produced significantly higher FPI scores (average of 25.8) relative to corresponding glacial *Cibicidoides* assemblages (average of 13.2) from 1.0 to 0 Ma (Figure 7b). Comparatively, all *Cibicidoides* assemblages in samples from the shallower deep North Atlantic Site 925 (3,052 m) produced relatively high FPI scores on average during both interglacial (FPI = 34.3) and glacial periods (FPI = 29.4), although interglacial assemblages were typically still slightly better preserved (Figure 7b).

Our sample coverage during the older timeslice for the deep North Atlantic sites is limited to the late Pliocene. Compared to *Cibicidoides* assemblages in samples from the deep Pacific Ocean during this timeslice (Figure 5c), those from the deep North Atlantic Sites 925 and 929 exhibit somewhat less variability (Figure 5d). Generally, interglacial *Cibicidoides* assemblages from Site 929 remain better preserved compared to

POIRIER ET AL. 12 of 32

2572425, 2021, 5, Downoladed from https://agupubs.onlinelibarry.wiley.com/doi/10.1029/2020PA004110, Wiley Online Library on [18/09/203]. See the Terms and Conditions (https://onlinelibarry.wiley.com/terms-and-conditions) on Wiley Online Library for rules of use; OA articles are governed by the applicable Creative Commons Licens

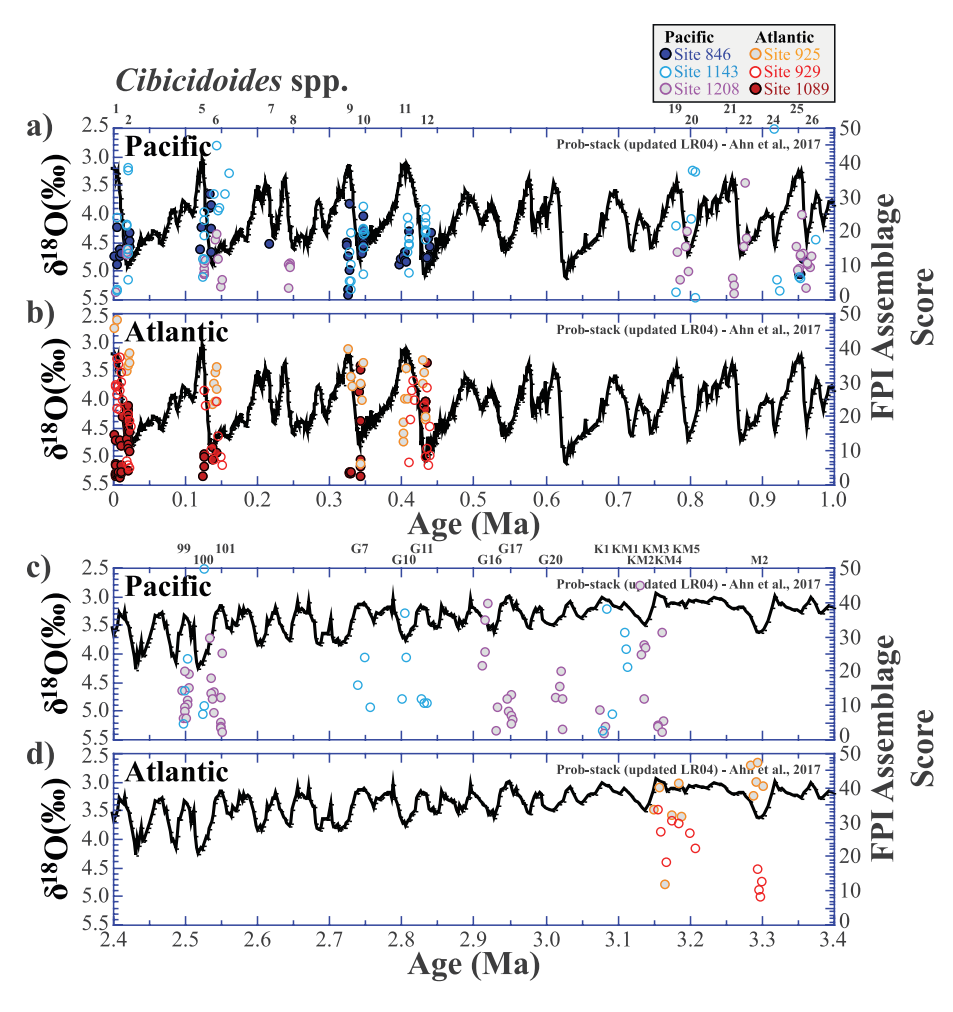


**Figure 5.** Peak interglacial and glacial Foraminiferal Preservation Index (FPI) scores for *Cibicidoides* assemblages from deep Atlantic (925: 3,052 m; 929: 4,356 m; 1089: 4,620 m) and deep Pacific (846: 3,296 m; 1143: 2,772 m; 1208: 3,346 m) sites (Table 1 and Figure 4) during the middle-to-late Pleistocene (a, b) and during the late Pliocene to early Pleistocene (c, d) study intervals. These FPI scores are compared to the updated global benthic  $\delta^{18}O$  stack of Ahn et al. (2017).

glacial *Cibicidoides* assemblages during MIS M2 (Figures 5d and 7a). In fact, average interglacial *Cibicidoides* assemblage FPI scores from the late Pliocene at Site 929 (FPI = 27.7) were comparable to those from the middle-to-late Pleistocene (FPI = 25.8) (Figure 7c). *Cibicidoides* assemblages in samples from Site 929 during the late Pliocene produced comparable average FPI scores during the M2 glacial as glacial assemblages from the middle-to-late Pleistocene, while average FPI scores from the KM4 glacial were notably higher (Figures 5 and 7a). Similarly, interglacial *Cibicidoides* assemblages from Site 925 were comparable during the late Pliocene (average FPI = 34.4) to those from the middle-to-late Pleistocene (average FPI = 34.3), while glacial assemblages produced higher FPI scores on average during the late Pliocene (FPI = 39.1) than during the middle-to-late Pleistocene (FPI = 29.4) (Figure 7). Interestingly, average *Cibicidoides* assemblage preservation quality in samples from the M2 glacial was slightly better than in assemblages from interglacial samples at Site 925 during the late Pliocene (Figure 7a).

# 4.1.2. Interglacial Versus Glacial *Uvigerina* Assemblage Preservation During the Middle-to-Late Pleistocene (1.0–0 Ma) and From the Late Pliocene to Early Pleistocene (3.4–2.4 Ma)

The same general FPI trends observed from *Cibicidoides* assemblages were also present in *Uvigerina* assemblages from deep Pacific Ocean and deep Atlantic Ocean samples during the middle-to-late Pleistocene and

POIRIER ET AL. 13 of 32

late Pliocene to early Pleistocene timeslices (Figures 6 and 7). *Uvigerina* assemblages from middle-to-late Pleistocene glacial periods produced higher FPI scores on average at deep Pacific Sites 846 (FPI = 17.7), 1143 (FPI = 22.0), and 1208 (FPI = 20.7), as well as the deep South Atlantic Site 1089 (FPI = 23.4), relative to those from interglacial periods (FPI = 12.0, 15.0, 14.4, and 17.4, respectively) (Figure 7b). Similarly, *Uvigerina* assemblages from the late Pliocene to early Pleistocene glacial periods produced higher average FPI scores at deep Pacific Sites 1143 (FPI = 15.8) and 1208 (FPI = 14.2) relative to those from interglacial periods (FPI = 8.5 and 11.1, respectively) (Figure 7c). As in the corresponding *Cibicidoides* assemblages from the same samples, there was a slightly higher degree of variability in *Uvigerina* assemblages from the older timeslice relative to the younger timeslice (Figure 6). Also similar to corresponding *Cibicidoides* assemblages, FPI scores in *Uvigerina* assemblage from glacial and interglacial samples at the deep North Atlantic Site 925 were comparable on average during both the middle-to-late Pleistocene (FPI = 22.6 and 21.0, respectively) and the late Pliocene to early Pleistocene (FPI = 19.0 and 19.3, respectively) (Figures 6 and 7). Unfortunately, only one *Uvigerina* specimen was present in any sample from the deep Atlantic Site 929. Therefore, comparison with trends in *Cibicidoides* assemblage FPI data from this location is not possible.

When comparing FPI data from the epifaunal *Cibicidoides* versus the infaunal *Uvigerina* assemblages from the deep Pacific and Atlantic Ocean samples, a few additional regional and temporal trends are noteworthy. First, middle-to-late Pleistocene glacial and interglacial *Uvigerina* assemblages from the deep Pacific Sites 846, 1143, and 1208, as well as the deep South Atlantic Site 1089, produced average FPI scores that were comparable or higher than corresponding *Cibicidoides* assemblages from the same samples (Figure 7b). This trend is most apparent in samples from Site 1143 and Site 1089. During the older late Pliocene to early Pleistocene interval, however, glacial and interglacial *Uvigerina* assemblages from Sites 1143 and 1208 produced comparable to lower average FPI scores on average relative to *Cibicidoides* assemblages (Figure 7c). Middle-to-late Pleistocene glacial and interglacial *Uvigerina* assemblages from the deep North Atlantic Site 925 produced lower FPI scores on average relative to corresponding *Cibicidoides* assemblages from the same samples (Figure 7b). This trend of lower average FPI scores from *Uvigerina* assemblages on average remains consistent at the deep North Atlantic Site 925 during the late Pliocene to early Pleistocene timeslice (Figure 7c).

#### 4.2. Water Mass Corrosivity as Driver of Regional and Temporal Trends in Preservation

Overall, the consistent trends discussed above cannot be explained by variations in sedimentation rate, nor by the sediment composition with regards to organic matter and CaCO<sub>3</sub> content (Table 1 and Section 3.1). While these factors likely contribute to assemblage preservation in some secondary capacity, the chemical properties, in particular the corrosivity, of the water masses present at each site at the time of deposition over glacial–interglacial cycles can explain all of the trends noted above. During interglacial periods of the middle-to-late Pleistocene, the only well-preserved *Cibicidoides* assemblages (i.e., with average FPI scores >15) were found at North Atlantic Sites 925 and 929 that are primarily bathed by the less corrosive north-ern-sourced NADW water mass during such times (Figure 7). Preservation quality at Site 925 remains just as high during late Pliocene interglacial periods, while improving slightly at Site 929. This could be related to the likelihood of AMOC being at least as strong and most likely stronger in the North Atlantic region during this time period relative to the middle-to-late Pleistocene (e.g., Dowsett et al., 2009, 2019).

A notable depth gradient in average FPI scores between North Atlantic Site 925 and Site 929 is an additional parameter demonstrating the influence of the northern-sourced NADW water mass on preservation quality (Figure 7). During both study intervals (Figure 7), interglacial *Cibicidoides* assemblages are best preserved at Site 925 (3,052 m, Figure 4), which resides at depths where core NADW waters dominate exclusively in the modern Holocene interglacial period (e.g., Oppo et al., 2018). Despite being well preserved on average, interglacial *Cibicidoides* assemblages at the deeper Site 929 are relatively less well preserved than those of the shallower Site 925 (Figure 7). This reduction in average *Cibicidoides* assemblage preservation quality reflects the moderate influence of southern-sourced AABW mixing with northern-sourced NADW at similar depths near Site 929 (4,356 m, Figure 4) in the modern ocean (e.g., Oppo et al., 2018).

This depth gradient in assemblage preservation quality between the North Atlantic sites 925 and 929 remains consistent during glacial periods. Glacial *Cibicidoides* assemblages at Site 925 are very well preserved, as regions of deepwater formation that coincide with the modern core of NADW likely remained active in

POIRIER ET AL. 14 of 32

2572425, 2021, 5, Downoladed from https://agupubs.onlinelibarry.wiley.com/doi/10.1029/2020PA004110, Wiley Online Library on [18/09/203]. See the Terms and Conditions (https://onlinelibarry.wiley.com/terms-and-conditions) on Wiley Online Library for rules of use; OA articles are governed by the applicable Creative Commons Licens

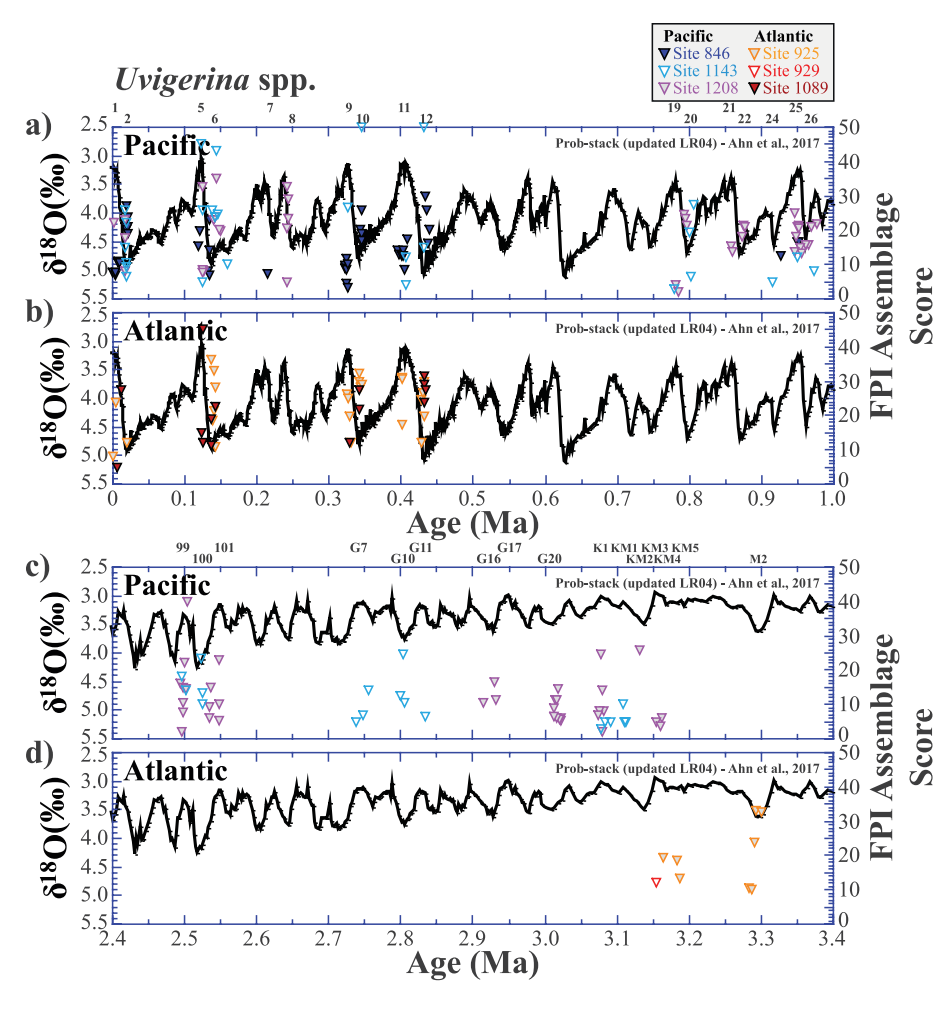


**Figure 6.** Peak interglacial and glacial Foraminiferal Preservation Index (FPI) scores for *Uvigerina* assemblages from deep Atlantic (925: 3,052 m; 929: 4,356 m; 1089: 4,620 m) and deep Pacific (846: 3,296 m; 1143: 2,772 m; 1208: 3,346 m) sites (Table 1 and Figure 4) during the middle-to-late Pleistocene (a, b) and during the late Pliocene to early Pleistocene (c, d) study intervals. These FPI scores are compared to the updated global benthic  $\delta^{18}O$  stack of Ahn et al. (2017).

the formation of GNAIW/GNADW during glacial periods (e.g., Oppo et al., 2018). Alternatively, regions in the northernmost North Atlantic and Arctic Oceans where the deeper and denser limb of NADW forms today were not active contributors to glacial AMOC. Instead, southern-sourced waters influenced a much larger proportion of the deep North Atlantic basin below depths of  $\sim$ 3,000–3,500 m in most glacial periods during the middle-to-late Pleistocene (e.g., Oppo et al., 2018; Poirier & Billups, 2014). This change in water mass influence at Site 929 corresponds with lower average glacial FPI scores during both intervals, similar to those at the deep North Pacific Site 1208 (Figure 7).

While only a single *Uvigerina* specimen was found in the samples from Site 929, *Uvigerina* assemblages from Site 925 were well preserved during both glacial and interglacial periods, on average (Figure 7). However, assemblages of this infaunal genus were typically less well preserved than corresponding epifaunal *Cibicidoides* assemblages at this site, regardless of climate state or study interval (Figure 7). This likely signifies that porewaters at Site 925 produced more corrosive microenvironments within the upper sediment column for *Uvigerina* specimens relative to that of NADW or GNAIW/GNADW through time.

Similar to the trends observed in the North Atlantic Ocean, the average preservation quality of *Cibicidoides* and *Uvigerina* assemblages from the Pacific Ocean through time likely coincides with dif-

POIRIER ET AL. 15 of 32

2572425, 2021, 5, Downloaded from https://agupubs.onlinelibarry.wiley.com/doi/10.1029/2020PA004110, Wiley Online Library on [18/09/2021]. See the Terms and Conditions (https://onlinelibarry.wiley.com/terms-and-conditions) on Wiley Online Library for rules of use; OA articles are governed by the applicable Creative Commons Licenses

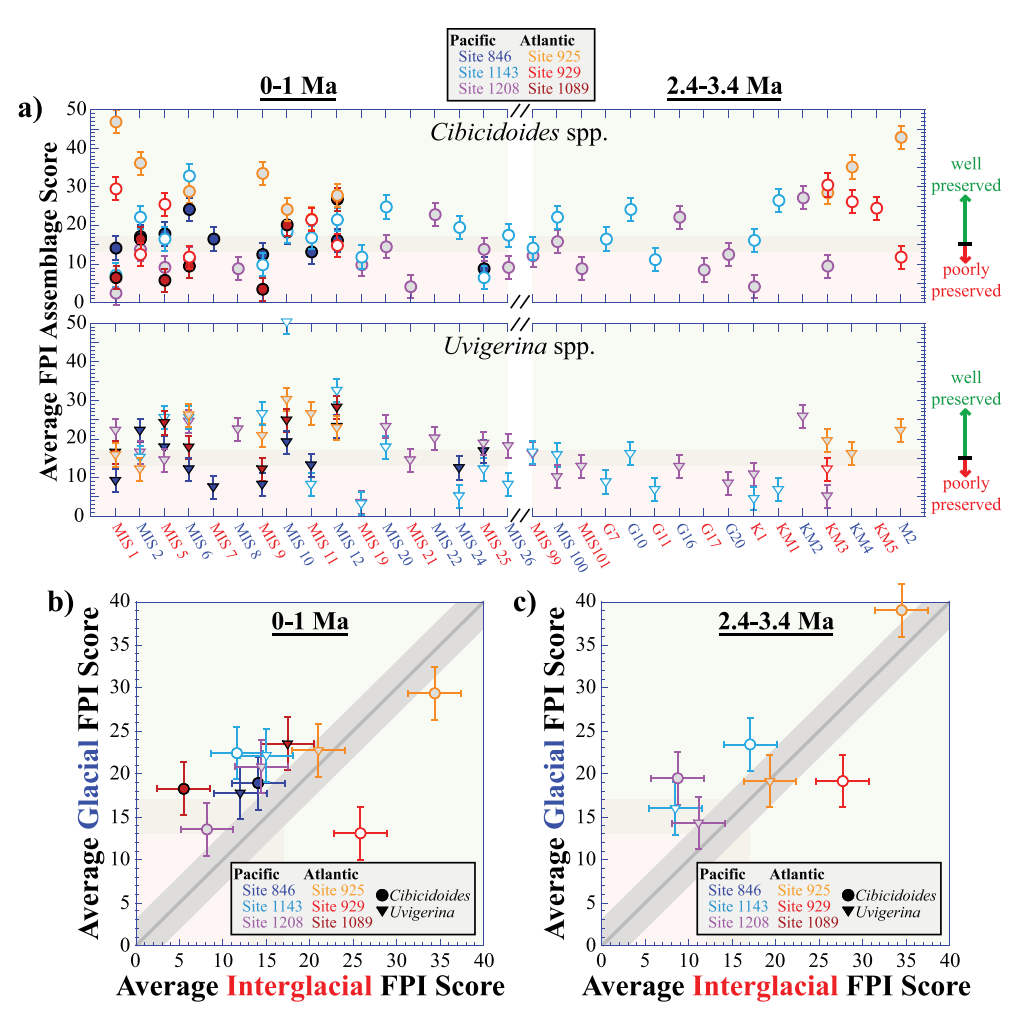


**Figure 7.** (a) Summary of average Foraminiferal Preservation Index (FPI) scores for *Cibicidoides* (color-coded circles) and *Uvigerina* (color-coded triangles) assemblages from each interglacial and glacial period studied herein. Average results from this summary demonstrate the relationship of average FPI assemblage preservation scores at each site during glacial versus interglacial periods during (b) the middle-to-late Pleistocene study interval and (c) the late Pliocene to early Pleistocene study interval. Error bars of  $\pm 3.1$  represent the approximate range of subjective variability for the FPI metric (Section 3.3).

ferential water mass influence over glacial cycles. The trend of better preserved assemblages during glacial periods relative to interglacial periods is consistent at each deep Pacific site, regardless of taxon (Figure 7). This suggests the influence of a less corrosive water mass relative to the modern interglacial PDW during glacial periods present in some proportion at depths between ~2,800 and 3,300 m. This finding corresponds with the influence of GNPIW in the deep Pacific Ocean, which is thought to have extended to water depths between ~2,000 and 3,000 m during the MIS 2 glacial period (e.g., Du et al., 2018; Herguera et al., 2010; Jian et al., 2003; Kwiek & Ravelo, 1999; Matsumoto et al., 2002; Okazaki et al., 2010). Unlike the modern nutrient-rich, relatively corrosive North Pacific Intermediate Water (NPIW) mass primarily influencing depths to ~1,500 m, the GNPIW had a higher carbon isotope signature indicative of lower nutrient concentrations than the glacial PDW and AABW (e.g., Lisiecki, 2014; Matsumoto et al., 2002). The depth gradient in preservation quality observed in glacial Cibicidoides assemblages (and to a less significant extent in glacial Uvigerina assemblages) suggests that the influence of GNPIW was higher at Site 1143 in the western deep Pacific basin than at slightly deeper depths of the central and eastern Pacific basins (Figure 4). This differential influence of GNPIW appears consistent during both the middle-to-late Pleistocene and late Pliocene to early Pleistocene study intervals, although to a lesser degree between ~3.4 and 2.4 Ma, on average (Figure 7).

POIRIER ET AL. 16 of 32

Middle-to-late Pleistocene interglacial preservation quality was moderate on average in *Cibicidoides* and *Uvigerina* assemblages at Pacific Sites 846 and 1143, as well as in *Uvigerina* assemblages from Site 1208, while *Cibicidoides* assemblages at Site 1208 were relatively poorly preserved (Figure 7). This suggests that the recirculating limb of PDW influencing depths of  $\sim$ 2,800–3,300 m in the eastern and western deep Pacific basins was slightly less corrosive than those at  $\sim$ 3,300 m beneath the Kuroshio extension in the central deep Pacific during interglacial periods over this interval. Compared to the younger timeslice, average interglacial *Cibicidoides* assemblage preservation was better at Site 1143 during the late Pliocene to early Pleistocene interval, while remaining more well preserved during glacial periods (Figure 7). This trend could be explained by a decreased influence of the AABW-sourced PDW in the eastern Pacific basin during interglacial periods in this interval relative to the deep central Pacific, where *Cibicidoides* assemblages from Site 1208 remained poorly preserved, on average (e.g., Kwiek & Ravelo, 1999). Interestingly, *Cibicidoides* assemblages at Site 1208 were typically better preserved on average during glacial periods in the  $\sim$ 3.4–2.4 Ma study interval than those of the middle-to-late Pleistocene (Figure 7), perhaps signifying a greater influence of GNPIW during the late Pliocene to early Pleistocene interval.

Compared to the average interglacial *Cibicidoides* assemblage preservation quality, average interglacial *Uvigerina* assemblage preservation was largely similar at Sites 846 and 1143 and significantly better at Site 1208 during the middle-to-late Pleistocene. This intertaxon trend is also consistent during glacial periods from ~1.0 to 0 Ma, suggesting that during this interval porewaters in the upper sediment column are similarly to less corrosive than the overlying dominant water mass in regions near Sites 846, 1143, and 1208. Despite *Uvigerina* assemblages from Site 1143 and Site 1208 still being moderately well preserved to poorly preserved on average during interglacial periods of the late Pliocene to early Pleistocene interval, they are unexpectedly less well preserved at both sites during glacial periods relative to corresponding *Cibicidoides* assemblages. This implies more corrosive porewaters relative to the PDW and GNPIW during glacial periods from the late Pliocene to early Pleistocene, perhaps resulting from a higher degree of organic carbon and CaCO<sub>3</sub> burial at the time (e.g., Bralower et al., 2002; Wang et al., 2000).

Results from the deep Pacific sites suggest a lower proportional influence of AABW at depths of ~2,800-3,300 m in the deep Pacific Ocean during glacial periods since ~3.4 Ma and possibly also during interglacial periods of the older late Pliocene to early Pleistocene interval (e.g., Sexton & Barker, 2012). Similar trends to those observed at the deep Pacific sites were also noted in the middle-to-late Pleistocene Cibicidoides and Uvigerina assemblages from the deep South Atlantic Site 1089 (Figure 7). On average, glacial assemblages are significantly better preserved than corresponding interglacial assemblages at Site 1089. While this site is likely bathed by southern source waters during both glacial and interglacial periods, it has been proposed that during glacial periods, a northward shift in the zone of deepwater formation in the South Atlantic and Southern Ocean may occur (e.g., Allen et al., 2015; Sikes et al., 2017; Ullermann et al., 2016). If correct, this might imply that the waters bathing Site 1089 shift from the most corrosive bottom waters of the AABW formed in the deepest basins surrounding Antarctica during interglacial periods to those formed farther north today and more akin to the Circumpolar Deep Water component of AABW or the Antarctic Intermediate Water, which are relatively less corrosive in the modern regime. However, a shift in the overall deepwater circulation regime from the Atlantic to Pacific during glacial periods might also result in less corrosivity at Site 1089 due to a possible buffering of carbonate ion concentrations resulting from increased dissolution in the North Atlantic basin (e.g., Broecker, 2006; Sexton & Barker, 2012; S. M. Sosdian et al., 2018). Regardless, the results from Site 1089 suggest the influence of a less corrosive water mass at the site during glacial periods. Relatively well-preserved *Uvigerina* assemblages during both glacial and interglacial periods of the middle-to-late Pleistocene interval at Site 1089 suggest that at all times, porewaters at this location are less corrosive than the overlying water mass. Less corrosivity in porewaters at Site 1089 relative to the overlying AABW may be related to the relatively high sedimentation rates (e.g., Gersonde et al., 1999).

Overall, all of the general trends discussed above from our various study sites are most likely linked to changes in water mass influence and associated changes in corrosivity. The FPI data from the North Atlantic Sites 925 and 929 are consistent with strong NADW influence during interglacial periods and with GNAIW/GNADW and AABW dominating at each site during glacial periods, respectively. The FPI data from the deep Pacific sites demonstrate influence of PDW during interglacial periods, with an increased

POIRIER ET AL. 17 of 32

2572425, 2021, 5, Downloaded from https://agupubs.onlinelibarry.wiley.com/doi/10.1029/2020PA004110, Wiley Online Library on [18/09/2021]. See the Terms and Conditions (https://onlinelibarry.wiley.com/terms-and-conditions) on Wiley Online Library for rules of use; OA articles are governed by the applicable Creative Commons Licenses

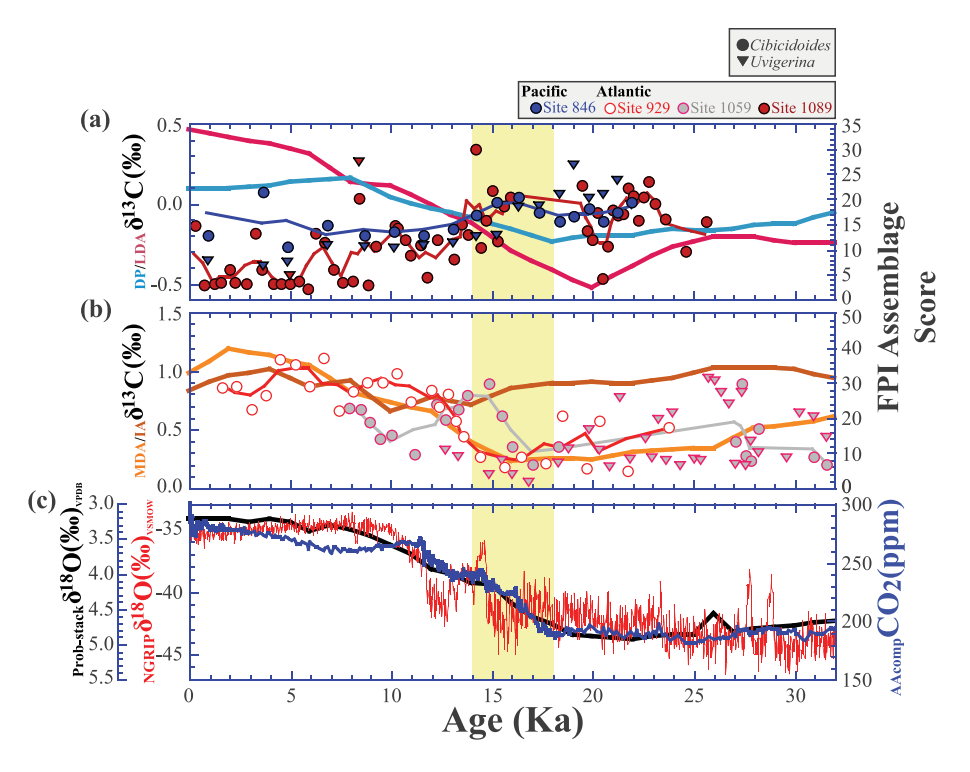


**Figure 8.** (a) Deglacial time series of Foraminiferal Preservation Index (FPI) scores for *Cibicidoides* and *Uvigerina* assemblages from various our deep Pacific and deep South Atlantic Ocean sites. These are compared to the regional  $\delta^{13}$ C stacks of Lisiecki (2014) from the deep Pacific (DP) and lower-deep Atlantic (LDA), respectively. Also shown are 3-pt moving averages of the *Cibicidoides* FPI scores (corresponding colors for each site). (b) Deglacial time series of FPI scores for *Cibicidoides* and *Uvigerina* assemblages from various our intermediate to deep North Atlantic Ocean sites. These are compared to the regional  $\delta^{13}$ C stacks of Lisiecki (2014) from the intermediate Atlantic (IA) and the middle-deep Atlantic (MDA), respectively. Also shown are 3-pt moving averages of the *Cibicidoides* FPI scores (corresponding colors for each site). (c) These records are compared to ice core records from Antarctica (Bereiter et al., 2015) and Greenland (Andersen et al., 2006; Rasmussen et al., 2006; Svensson et al., 2006, 2008; Vinther et al., 2006), as well as the updated global benthic  $\delta^{18}$ O stack (Ahn et al., 2017). Yellow vertical bar highlights the period of preservation changes for all sites between ~18 and 14 ka.

glacial influence of the less corrosive GNPIW particularly in the western Pacific basin near Site 1143. The middle-to-late Pleistocene FPI records generated from Site 1089 are consistent with an influence of AABW similar to modern during interglacial periods, while the AABW present at the site during glacial periods was less corrosive. This may represent a change in source water, carbonate buffering, or a combination of both. Finally, the relationship between average preservation of infaunal *Uvigerina* assemblages relative to those of the epifaunal *Cibicidoides* genera likely reflects variations in corrosivity between the deepwater masses influencing any given site relative to porewaters circulating through the underlying sediments at the time of deposition. Below, we discuss our FPI time series through the last deglaciation testing our conclusion that changes in assemblage preservation are most likely driven by changes in water mass chemistry through time (e.g., Bostock et al., 2011, 2013).

#### 4.3. Assemblage Preservation and Deepwater Mass Circulation During the Last Deglaciation

We interpret major trends in our FPI results as being associated with changes in water mass properties. To test this interpretation, we generated high-resolution FPI results from four sites spanning the last deglaciation. This transitional time period has been extensively studied, with major changes in atmospheric temperature,  $CO_2$  concentration, and deep-ocean circulation occurring during the ~18–14 ka interval (e.g., Andersen et al., 2006; Barker et al., 2009, 2010; Bereiter et al., 2015; Böhm et al., 2015; Burke & Robinson, 2012; Chen et al., 2015; Chowdhry Beeman et al., 2019; Clark et al., 2012; Ezat et al., 2017; Gray

POIRIER ET AL. 18 of 32

et al., 2020; Lund et al., 2015; Martínez-Botí et al., 2015; McManus et al., 2004; Mulitza et al., 2017; Rasmussen et al., 2006; Ronge et al., 2016; Sikes et al., 2016; Skinner et al., 2015; Svensson et al., 2006, 2008; Vinther et al., 2006; Zhang et al., 2017). Therefore, if our interpretation of the FPI results being associated with the corrosivity of different water masses during glacial versus interglacial periods is correct, changes in FPI assemblage preservation scores should occur at  $\sim$ 18–14 ka in the deep North Atlantic (i.e., at Sites 929 and 1059), South Atlantic (i.e., at Site 1089), and Pacific Oceans (i.e., at Site 846). From these sites, we applied the FPI metric to *Cibicidoides* (n = 126) and *Uvigerina* (n = 55) assemblages spanning the last deglaciation from sediment samples with an average sampling resolution of 688 years (average resolution ranged from 346 to 1,167 years for individual sites). This sampling resolution was calculated based on the age model of Lisiecki and Raymo (2005) for all sites except Site 1059, for which we used the published age model of Hagen and Keigwin (2002) that was generated using radiocarbon dates from planktic foraminifera.

In addition to interglacial and glacial FPI data corresponding with the broader trends documented throughout the middle-to-late Pleistocene (Section 4.1), the amplitude of FPI scores at each site varies similarly to relevant regional  $\delta^{13}$ C stacks recording average water mass signatures during the Holocene and MIS 2 (Figure 8). The average amplitude of change in FPI scores from MIS 1 versus MIS 2 ([ΔFPI<sub>MIS 1-2</sub>]) at the deep North Atlantic Site 929 ( $[\Delta FPI_{MIS 1-2}] = 16.9$ ) and the deep South Atlantic Site 1089 ( $[\Delta FPI_{MIS 1-2}] = 9.1$ ) is larger relative to the more intermediate Atlantic (IA) Site 1059 ([ $\Delta FPI_{MIS 1-2}$ ] = 6.1) and the deep Pacific Site 846 ( $[\Delta FPI_{MIS 1-2}] = 7.9$ ), respectively. This observation coincides with similar trends in the amplitude of changes in regional  $\delta^{13}$ C stacks of Lisiecki (2014), where larger changes in average  $\delta^{13}$ C from MIS 1 versus MIS 2 ([ $\Delta\delta^{13}C_{MIS\,1-2}$ ]) occur in the middle-deep Atlantic (MDA) and lower-deep Atlantic (LDA)  $\delta^{13}C$  stacks  $([\Delta \delta^{13}C_{MIS,1-2}]: MDA = 0.699; LDA = 0.689)$ , which essentially record average  $\delta^{13}C$  values in the regions influenced primarily by the lower limb of the NADW and the AABW, respectively (Figure 8). In contrast, relatively small  $[\Delta \delta^{13}C_{MIS\,1-2}]$  is recorded by the IA and deep Pacific (DP) regional  $\delta^{13}C$  stacks  $([\Delta \delta^{13}C_{MIS\,1-2}]$ : IA = 0.028; DP = 0.304), which record average interglacial/glacial  $\delta^{13}$ C values for the core NADW/GNAIW/ GNADW and the PDW/GNPIW, respectively (Figure 8). These regional similarities along with the timing of changes in FPI assemblage scores support our interpretation that water mass chemistry is the primary influence on assemblage preservation quality through time.

The timing of changes in FPI scores occurs at each site within the expected ~18–14 ka interval (Figure 8). Notably, decreases in FPI scores appear synchronous at the deep Pacific Site 846 and the deep South Atlantic Site 1089 beginning at ~17–15 ka (Figure 8a). The timing of this change broadly coincides with Heinrich Stadial 1 (HS1) and the notable increase in  $CO_2$  concentrations measured in Antarctica, just prior to the Northern Hemisphere Bølling-Allerød warming event associated with Meltwater Pulse (MP) 1A (Figure 8c). The timing of changes in FPI assemblage scores also coincides with increasing  $\delta^{13}C$  in the DP and LDA regional stacks, likely as a function of both changes in deep-ocean circulation and outgassing of isotopically light  $CO_2$  to the atmosphere (e.g., Burke & Robinson, 2012; Chen et al., 2015; Clark et al., 2012; Gray et al., 2020; Martínez-Botí et al., 2015; Ronge et al., 2016; Sikes et al., 2016). In the early Holocene, FPI scores appear to stabilize at Site 846 by ~9–8 ka, whereas they continue to decrease until ~7–6 ka at Site 1089, similar to changes in  $\delta^{13}C$  in the DP and LDA regional stacks, respectively (Figure 8a). Overall, changes in FPI scores at Site 846 and Site 1089 appear consistent with corresponding regional  $\delta^{13}C$  stacks reflecting decreased influence of GNPIW and increased influence of AABW throughout the deep Pacific and South Atlantic Oceans, as well as outgassing of  $CO_2$ . Ultimately, these changes are also in general agreement with ice core records from the northern and southern hemispheres (Figure 8c).

Similar to the deglacial FPI time series from the deep Pacific and South Atlantic Oceans, the timing of changes in assemblage preservation at the deep North Atlantic Sites 929 and 1059 coincides with changes in deep circulation and atmospheric events (Figure 8b). Increases in FPI scores begin at ~17–15 ka at Site 1059, which samples core NADW and the approximate boundary between GNAIW/GNADW and AABW during MIS 1 and MIS 2, respectively. This timing appears more similar to that from the deep Pacific and South Atlantic sites, perhaps related to HS1, and coincides with a  $\delta^{13}$ C decrease of 0.138% in the IA regional  $\delta^{13}$ C stack of Lisiecki (2014). During the ~14–10 ka interval, Site 1059 FPI scores decrease, accompanied by an additional  $\delta^{13}$ C decrease of 0.059% in the IA regional  $\delta^{13}$ C stack. These changes could indicate with a weakening of NADW formation in the North Atlantic source region during the Younger Dryas Northern

POIRIER ET AL. 19 of 32

2572425, 2021, 5, Downloaded from https://agupubs.onlinelibarry.wiley.com/doi/10.1029/2020PA004110, Wiley Online Library on [18/09/2021]. See the Terms and Conditions (https://onlinelibarry.wiley.com/terms-and-conditions) on Wiley Online Library for rules of use; OA articles are governed by the applicable Creative Commons Licenses

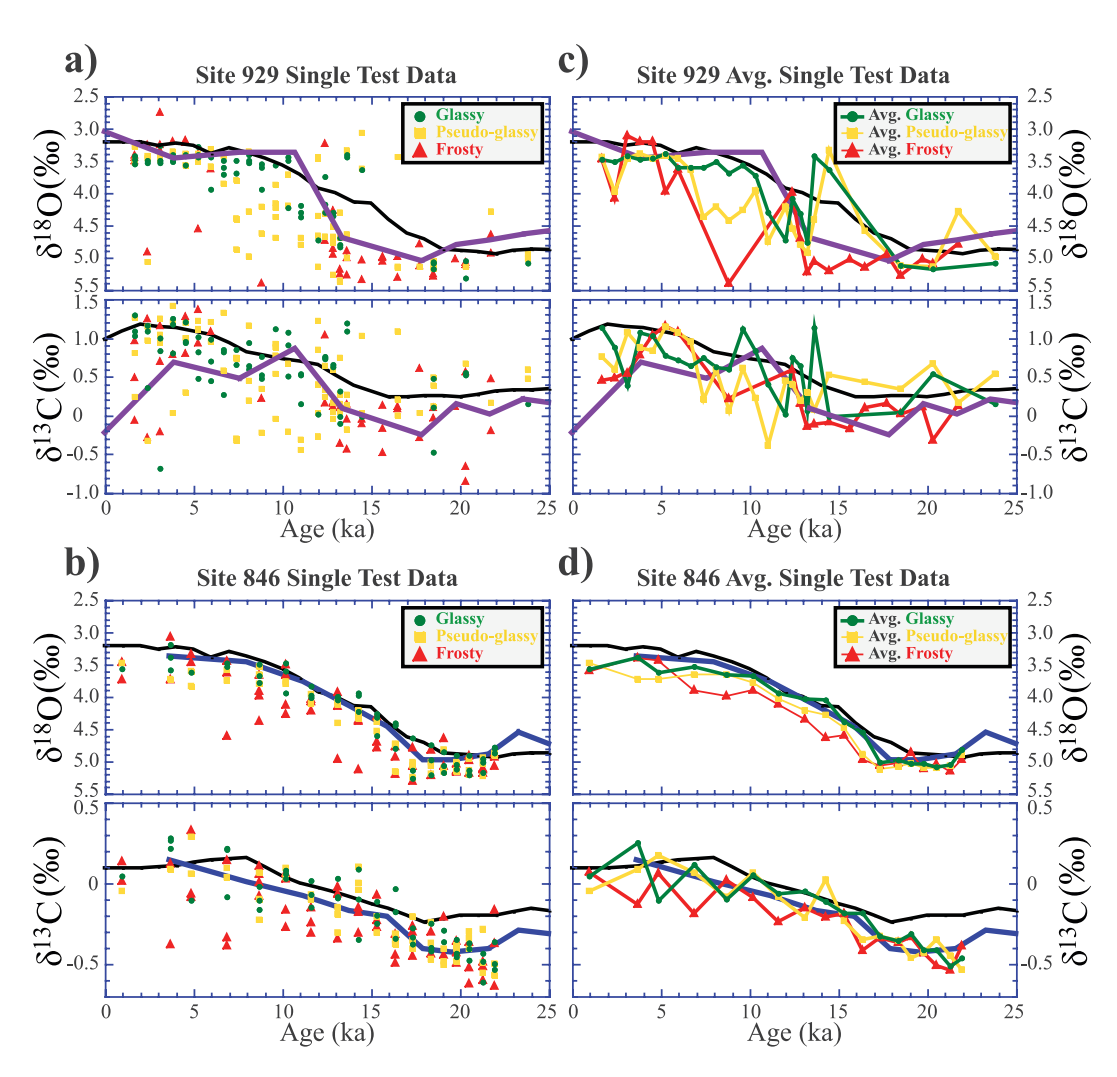


Figure 9. Single-test stable isotope results from *Cibicidoides* specimens of each preservation state (color and shape coded) at (a) the deep North Atlantic Site 929 and (b) the deep Pacific Site 846. To quantify isotopic offsets between data generated from tests of each preservation state in each individual assemblage (Figure 10), average time series for each preservation state are also shown for data from (c) Site 929 and (d) Site 846. The solid purple time series in panels (a) and (c) is the published stable isotope data from Site 929 of Bickert et al. (1997). The solid blue time series in panels (b) and (d) is the published stable isotope data from Site 846 of Mix et al. (1995). The solid black  $\delta^{18}$ O time series is the Prob-stack data of Ahn et al. (2017), which expanded upon the LR04 stack of Lisiecki and Raymo (2005). The solid black  $\delta^{13}$ C time series in panels (a) and (c) and in panels (b) and (d) are the middle-deep Atlantic and the Deep Pacific regional stacks of Lisiecki (2014), respectively.

Hemisphere cooling event (Figure 8c). After  $\sim$ 10 ka, Site 1059 FPI scores increase again into the Holocene, corresponding with an increase in the IA regional  $\delta^{13}$ C stack (Figure 8b). These changes in assemblage preservation at the more intermediate Site 1059 do not occur simultaneously with those from the deep North Atlantic Site 929.

Assemblage FPI scores at Site 929 stay relatively low until ~15–14 ka, when a steady increase in FPI scores continues into the early Holocene, followed by a second slight increase in preservation scores during the middle Holocene (Figure 8b). The timing of changes in preservation at Site 929 coincides with synchronous changes in the MDA regional  $\delta^{13}C$  stack. These two records relate almost exclusively to the onset of strong AMOC, which generally began after HS1, corresponding with the onset of the Bølling-Allerød warming and  $CO_2$  outgassing events associated with MP-1A (e.g., Barker et al., 2010; Böhm et al., 2015; Chen et al., 2015; Clark et al., 2012; Ezat et al., 2017; Lund et al., 2015; McManus et al., 2004). The difference in timing between the more intermediate Site 1059 and the deeper Site 929 may support the recent

POIRIER ET AL. 20 of 32

2572425, 2021, 5, Downloaded from https://agupub.son/inelibarry.wiley.com/doi/10.1029/2020PA004110, Wiley Online Library on [18/09/203]. See the Terms and Conditions (https://onlinelibarry.wiley.com/terms-and-conditions) on Wiley Online Library for rules of use; OA articles are governed by the applicable Creative Commons Licensia.

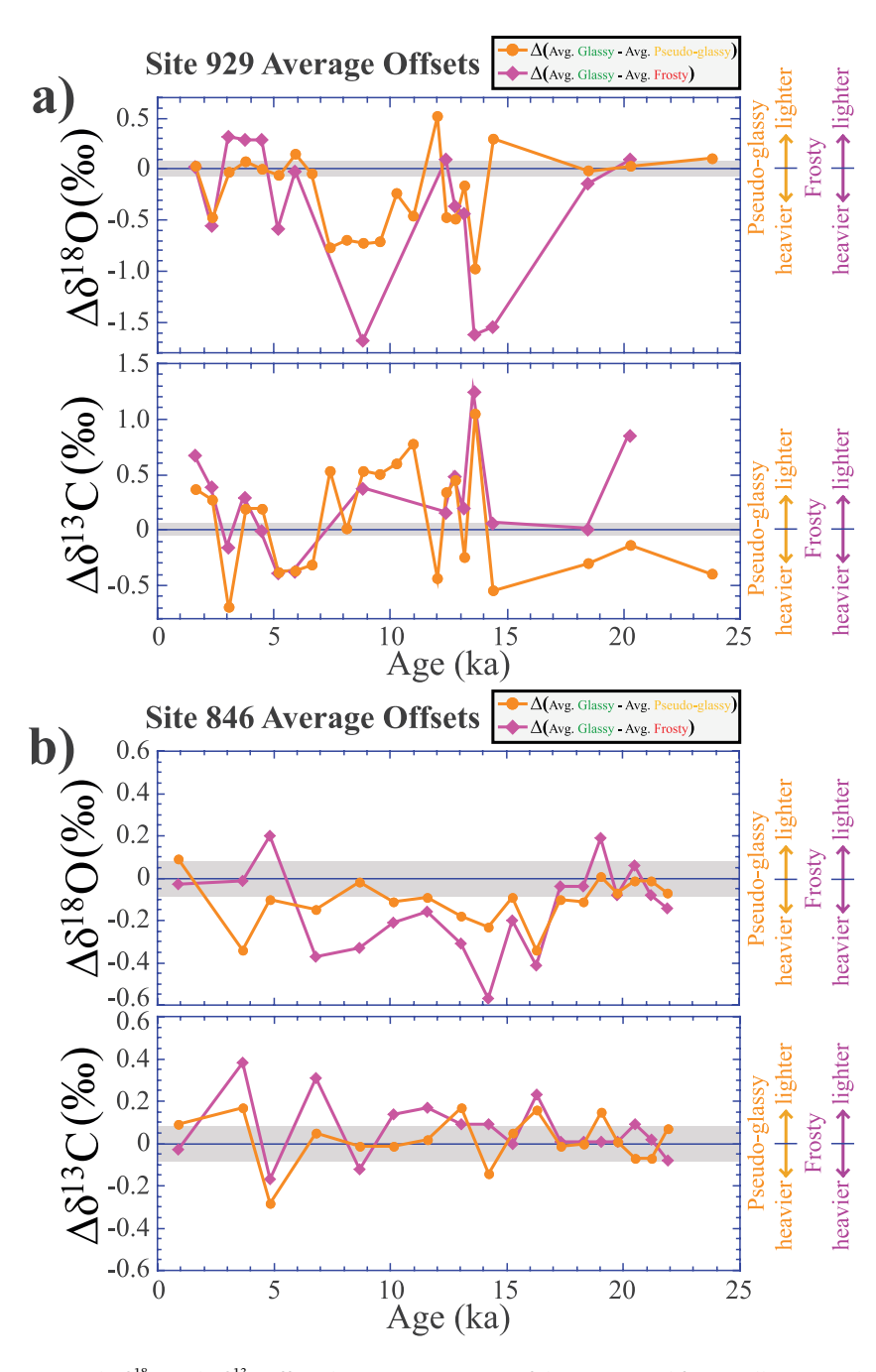


Figure 10. Temporal  $\Delta\delta^{18}O$  and  $\Delta\delta^{13}C$  offsets between time series of data generated from well-preserved glassy *Cibicidoides* specimens relative to corresponding data from altered pseudo-glassy (orange) and frosty (purple) specimens from (a) Site 929 and (b) Site 846. Horizontal gray bars represent the range of data offsets that are likely negligible based on our achieved analytical precision of better than 0.08% for  $\delta^{18}O$  and 0.06% for  $\delta^{13}C$ .

modeling of Zhang et al. (2017), which suggests early middepth warming in the deep North Atlantic preceded changes in the deep South Atlantic during periods when AMOC was generally reduced, such as in HS1.

In all, the deglacial FPI results from Sites 846, 929, 1059, and 1089 support our interpretation that changes in assemblage preservation quality are primarily controlled by water mass chemistry. The corrosivity

POIRIER ET AL. 21 of 32

of the water mass present at any given site therefore is the primary driver of the dissolution we observe within specific domains of the internal chamber walls in these benthic taxa (Section 2.2; Figures 2 and 3), ultimately resulting in the proportion of well-preserved versus altered tests in any given sediment sample. Furthermore, the deglacial FPI time series from these sites demonstrates the applicability of this metric as a qualitative and quantitative deep-ocean circulation proxy to complement other records in the future. The deglacial FPI data document changes in the intermediate-deep North Atlantic Ocean coinciding with or perhaps slightly leading changes in the deep South Atlantic and Pacific Oceans associated with HS1. Following these preservation changes in the intermediate-deep North Atlantic, the deep South Atlantic, and the deep Pacific, changes in assemblage preservation initiated in the deepest region of the North Atlantic Ocean at the onset of the Bølling-Allerød warming event, associated with MP-1A. Trends in each record coincide with the corresponding regional  $\delta^{13}$ C stacks of Lisiecki (2014) throughout the deglaciation, as well as during the early-to-middle Holocene.

#### 4.4. Quantifying Potential Diagenetic Biasing in Stable Isotope Records

#### 4.4.1. Single-Test Stable Isotope Analyses

To quantify the potential effect of diagenetic biasing that might occur in the most commonly generated geochemical proxy records, we generated single-test stable isotope data from Cibicidoides specimens of each preservation state, collected from samples recovered at Pacific Site 846 (n = 148) and at Atlantic Sites 929 (n = 172) and 1089 (n = 109) spanning the last deglaciation. These included stable isotope analyses of Cibicidoides wuellerstorfi (n = 384) and Cibicidoides mundulus (n = 45) specimens. From 33 paired analyses between glassy tests of these two species, we found no significant offset in  $\delta^{18}$ O but noted an offset correction between the two species for  $\delta^{13}$ C of 0.216 and 0.491 during late deglacial to interglacial (i.e., ~15–0 ka) and glacial to early deglacial periods (i.e.,  $\sim$ 25–15 ka), respectively. These offsets, which we added to each C. mundulus  $\delta^{13}$ C measurement, were similar to those found by Gottschalk et al. (2016) from sites in the deep South Atlantic Ocean. Finally, we applied the Cibicidoides offset correction of 0.64% documented by N. J. Shackleton et al. (1984) to all  $\delta^{18}$ O data. Results from Sites 846 and 929 are illustrated in Figures 9 and 10. All of the deglacial results, including those from Site 1089 and for MIS 9–10 from Site 846 (n = 34), are provided in the Supporting Information and can also be found online at the PANGAEA data repository. While the observed trends from the deglacial Site 1089 data generally align with the interpretation from Sites 846 and 929 discussed below (Figures S1 and S2 in the Supporting Information), the number of tests of each preservation state available for analysis was inadequate to quantify the results in a comparable way and is therefore not discussed further.

From Sites 846 and 929, we generated single-test stable isotope data throughout the last deglaciation from three individual tests of each preservation state (Figures 9a and 9b) that were picked from the same sediment sample (i.e., assemblage), whenever possible. Images of each test analyzed from these two sites during the last deglaciation are included within Plates S7–S53 of the Supporting Information. Several observations are apparent in the single-test data from each site: first, glassy tests from within the same sample typically produce stable isotope data that are relatively reproducible compared to that from altered tests, with average maximum variance of 0.292%/0.176% and 0.240%/0.487% among glassy *Cibicidoides* tests analyzed for  $\delta^{18}$ O/ $\delta^{13}$ C from the same samples at Site 846 (n=16) and Site 929 (n=19), respectively. Reproducibility of single-test stable isotope data generated from pseudo-glassy tests was similar at Site 846 and substantially worse at Site 929, while reproducibility of frosty tests from the same samples was substantially worse at both sites. Average maximum variance of 0.207%/0.137% and 0.691%/0.740% was measured from pseudo-glassy *Cibicidoides* specimens analyzed for  $\delta^{18}$ O/ $\delta^{13}$ C from the same samples at Site 846 (n=16) and Site 929 (n=23), respectively. Finally, the average maximum variance of 0.474%/0.258% and 0.473%/0.663% was measured from frosty *Cibicidoides* specimens analyzed for  $\delta^{18}$ O/ $\delta^{13}$ C from the same samples at Site 846 (n=16), respectively.

These observations identify a wider degree of variance among  $\delta^{13}C$  data relative to  $\delta^{18}O$  at Site 929 during this interval, regardless of preservation state, while not being evident at Site 846. The  $\delta^{13}C$  composition of benthic foraminifera generally reflects that of the overlying water masses (i.e., within the modern regime: higher  $\delta^{13}C$  for nutrient depleted NADW; lower  $\delta^{13}C$  for nutrient enriched AABW) and therefore can be sub-

POIRIER ET AL. 22 of 32

ject to more variance at sites located near mixing zones of different water masses such as Site 929. Furthermore, various processes at both sites, including in situ respiration of organic matter at the sediment–water interface (e.g., Mackensen et al., 1993; Zarriess & Mackensen, 2011), can also contribute to variance within  $\delta^{13}$ C data generated from benthic foraminifera.

The second major observed trend is that single-test stable isotope data generated from altered pseudo-glassy and frosty tests produced higher average  $\delta^{18}O$  and lower average  $\delta^{13}C$  values than glassy tests (Figure 10). Data from pseudo-glassy tests from Site 929 were 0.218% higher and 0.092% lower on average relative to  $\delta^{18}O$  and  $\delta^{13}C$  data generated from glassy tests collected within the same sample, respectively. Frosty tests from Site 929 were 0.390% higher and 0.251% lower on average relative to glassy tests from the same sample, respectively. Similar offsets were also noted in the Site 846 data, albeit to a lesser degree. Data from pseudo-glassy tests from Site 846 were 0.107% higher and 0.020% lower on average relative to  $\delta^{18}O$  and  $\delta^{13}C$  data generated from glassy tests collected within the same sample, respectively. Frosty tests from Site 846 were 0.140% higher and 0.064% lower on average relative to glassy tests from the same sample, respectively.

Finally, results from both sites demonstrate that the most variability between ideally preserved glassy tests and altered pseudo-glassy and frosty tests occurs during the  $\sim$ 17–6 ka interval, from the early phase of deglaciation into the middle Holocene (Figures 9 and 10). These three observations are most apparent when averaging the single-test results from each preservation state within each sample, thereby creating individual stable isotope time series-records for glassy, pseudo-glassy, and frosty tests (Figures 9c and 9d). While these time series generally overlap with the published low-resolution records from each site (i.e., Bickert et al., 1997; Mix et al., 1995), periods of notable offsets between those records and the glassy time series are evident. These offsets likely relate to sampling resolution in some cases and diagenetic biasing in others. Regardless, compiling the single-test stable isotope data into a time series record for each preservation state allows us to quantify the average stable isotope composition offsets through time.

From each sample/assemblage, we subtract the average pseudo-glassy and frosty stable isotope values from the corresponding average glassy values (Figure 10). The resulting  $\Delta \delta^{18}O$  and  $\Delta \delta^{13}C$  time series for each site again demonstrate similar offset trends throughout the various time series at both sites. From MIS 2 to the early deglaciation (i.e.,  $\sim 25-17$  ka),  $\Delta \delta^{18}$ O and  $\Delta \delta^{13}$ C offsets between well-preserved and diagenetically altered tests are generally negligible at Site 846 compared to our achieved analytical precision (Section 3.4): 0.019%-0.051% and 0.010%-0.011%, respectively, and at Site 929: 0.021%-0.041% and 0.071%-0.286%, respectively. Throughout the remainder of the deglacial period and the early-to-middle Holocene (i.e., ~17– 6 ka), the  $\Delta \delta^{18}$ O and  $\Delta \delta^{13}$ C offsets at both sites increase significantly with altered tests generally exhibiting higher  $\delta^{18}$ O and lower  $\delta^{13}$ C values. Average  $\Delta\delta^{18}$ O and  $\Delta\delta^{13}$ C offsets during this interval were respectively: 0.151‰-0.320% and 0.036%-0.114% at Site 846; 0.316%-0.406% and 0.120%-0.311% at Site 929. While these average offsets are problematic themselves with regards to proxy records, isotopic offsets between average glassy and average pseudo-glassy tests within individual samples/assemblages varied in  $\Delta \delta^{18}$ O/  $\Delta \delta^{13}$ C by up to 0.340%/0.170% at Site 846 and by up to 0.977%/1.056% at Site 929 during this interval. Similarly, isotopic offsets between average glassy and average frosty tests within individual samples/assemblages varied in  $\Delta\delta^{18}$ O/ $\Delta\delta^{13}$ C by up to 0.570%/0.230% at Site 846 and by up to 1.685%/1.244% at Site 929 during this interval. During the middle-to-late Holocene (i.e.,  $\sim$ 6-0 ka), offsets in  $\Delta\delta^{18}$ O and  $\Delta\delta^{13}$ C between well-preserved glassy relative to altered pseudo-glassy and frosty tests reduce to 0.053%-0.117% and 0.007%-0.060% on average at Site 846, respectively, and to 0.007%-0.037% and 0.085%-0.087% on average at Site 929, respectively. These middle-to-late Holocene offsets are again relatively negligible, compared to our achieved analytical precision (Figure 10 and Section 3.4).

Overall, these single-test results and the corresponding  $\Delta\delta^{18}O$  and  $\Delta\delta^{13}C$  offsets have two major implications: first, regarding the potential for diagenetic biasing of isotopic data resulting from the incorporation of altered tests in pooled geochemical analyses; and second, regarding the diagenetic processes that might explain the temporally distinct isotopic offsets between altered and pristine tests. As demonstrated within this data set, the inclusion of even a single pseudo-glassy or frosty test in a pooled geochemical analysis is sufficient to bias the resulting data. Furthermore, in some instances, the offset between average stable isotope data from glassy and pseudo-glassy tests is more significant than that between glassy and frosty tests (e.g.,  $\delta^{18}O_{929}$ : at 5.9 ka and 12.4–12.8 ka;  $\delta^{13}C_{929}$ : at 3.0 ka, 4.5 ka, 7.4–12.4 ka, and 14.4–18.5 ka;  $\delta^{18}O_{846}$ : at 0.9–3.7 ka and 17.3–18.3 ka;  $\delta^{13}C_{846}$ :at 0.9 ka, 4.8 ka, 13.0–14.2 ka, 19.0 ka, and 21.2 ka—Figure 10). This

POIRIER ET AL. 23 of 32

2572425, 2021, 5, Downloaded from https://agupub.os.nlinelibarry.wiley.com/doi/10.1029/2020PA004110, Wiley Online Library on [18/09/2021]. See the Terms and Conditions (https://onlinelibrary.wiley.com/terms-and-conditions) on Wiley Online Library for rules of use; OA articles are governed by the applicable Creative Commons Licens

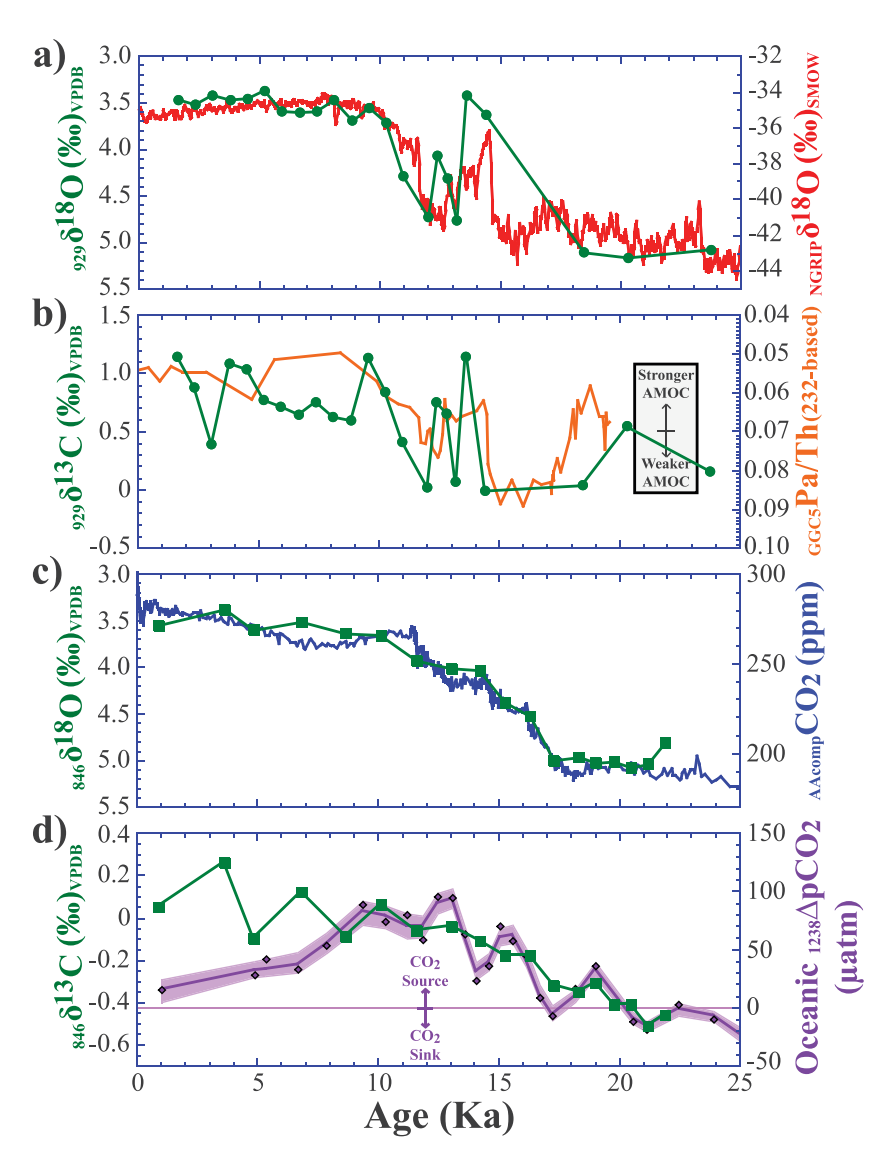


**Figure 11.** Comparisons of robust stable isotope data generated exclusively from well-preserved glassy *Cibicidoides* specimens from Site 929 compared to (a) the NGRIP ice core record (Andersen et al., 2006; Rasmussen et al., 2006; Svensson et al., 2006; 2008; Vinther et al., 2006) and (b) the Pa/Th record from the GGC5 site on the Bermuda Rise of McManus et al. (2004) and from Site 846 compared to (c) the Antarctic composite ice core  $CO_2$  record (Bereiter et al., 2015) and (d) the surface ocean  $\Delta pCO_2$  record from Site 1238 (Martínez-Botí et al., 2015).

observation demonstrates that while pseudo-glassy tests likely bias geochemical data to a lesser degree relative to frosty tests on average, they should also be avoided for the generation of robust proxy records. While difficult to constrain or assess, this biasing is likely a problem in many published stable isotope records using pooled-test analyses (Section 5).

It is notable that the time period from the early deglaciation to the middle Holocene exhibits the most pronounced offsets between records generated from well-preserved glassy tests and those from altered pseudo-glassy and frosty tests at both sites (Figure 10). This suggests that geochemical proxy records generated from pooled-test analyses during deglaciations and early interglacial periods may be the most susceptible periods to substantial isotopic biasing driven by diagenesis. For example, such biasing could lead to inaccurate reconstructions of past sea level and ice volume during deglaciations and early interglacial periods (i.e., the first  $\sim$ 5 kyr), which are often based at least in part on stable isotope data similar to that generated here. Our results indicate that reconstructions of past sea level derived from deep-sea benthic stable iso-

POIRIER ET AL. 24 of 32

 Table 2

 Number of Assemblages Producing Sufficient Glassy Specimens for Robust Pooled Geochemical Analyses

IODP site	Cibicidoides assemblages studied	Assemblages with ≥3 glassy Cibicidoides specimens	Assemblages with ≥10 glassy Cibicidoides specimens	Uvigerina assemblages studied	Assemblages with ≥3 glassy Uvigerina specimens	Assemblages with ≥10 glassy <i>Uvigerina</i> specimens
846	54	42 (77.8%)	18 (33.3%)	54	42 (77.8%)	25 (46.3%)
925	42	33 (78.6%)	3 (7.1%)	33	15 (45.5%)	5 (15.2%)
929	59	32 (54.2%)	16 (27.1%)	1	0 (0.0%)	0 (0.0%)
1059 <sup>a</sup>	23	9 (39.1%)	3 (13.0%)	34	7 (20.6%)	1 (2.9%)
1089	82	13 (15.9%)	0 (0.0%)	17	3 (17.6%)	0 (0.0%)
1143	85	29 (34.1%)	2 (2.4%)	46	7 (15.2%)	3 (6.5%)
1208	96	35 (36.5%)	2 (2.1%)	79	36 (45.6%)	17 (21.5%)
<u>Total:</u>	<u>441</u>	<u>193 (43.7%)</u>	<u>44 (10.0%)</u>	<u>264</u>	<u>110 (41.7%)</u>	<u>51 (19.3%)</u>

<sup>a</sup>Site only studied for the last deglaciation.

tope records during early interglacial periods are most likely biased toward lower sea-level estimates based on altered tests generating significantly higher  $\delta^{18}O$  values relative to well-preserved tests. This diagenetic biasing is also potentially significant during other periods of major climatic change, including transitions between stadial and interstadial periods, in addition to relatively rapid glacial/stadial inceptions. The net effect of such biasing would be to delay the true signal of climatic change, regardless of the direction of the shift.

In addition to the possibility of diagenetic biasing potentially affecting long-term paleo-sea-level reconstructions, these results are particularly important to modeling studies that incorporate parameters based on such proxy reconstructions. For example, misinterpretation of peak sea level during the early stages of key interglacial periods of the middle-to-late Pleistocene (i.e., MIS 5e and 11) based on even slightly biased proxy records could have cascading effects relevant to modeling future sea levels. Ultimately, these potential consequences of diagenetic biasing are supported by our interpretation of the underlying processes most likely resulting in the temporally distinct isotopic offsets between well-preserved glassy tests relative to altered pseudo-glassy and frosty tests.

#### 4.4.2. Diagenetic Processes Contributing to Documented Isotopic Offsets

Three possible explanations must be considered to explain the documented offsets in stable isotope results between well-preserved versus altered tests during the last deglaciation: (1) extensive reworking of older fossil tests into deglacial and early-to-middle Holocene sediments (i.e., with higher  $\delta^{18}$ O and lower  $\delta^{13}$ C shell composition); (2) isotope fractionation during dissolution of various domains within altered tests; or (3) inorganic calcite recrystallization occurring in concert with dissolution during alteration, potentially involving multiple dissolution–reprecipitation cycles. Reworking of older fossil tests is a common occurrence; however, this should be a relatively random phenomenon at any given site, driven by bioturbation. Due to the similarity in timing ( $\sim$ 17–6 ka), as well as the range of these isotopic offsets between well-preserved and altered tests at both sites, bioturbation seems unlikely (e.g., Wycech et al., 2016).

A second possible explanation of isotopic fractionation during the dissolution of internal chamber wall materials in *Cibicidoides* is also unlikely. As altered tests feature higher  $\delta^{18}O$  and lower  $\delta^{13}C$  values relative to well-preserved tests, on average, fractionation that could explain these observations requires preferential dissolution of the lighter  $^{16}O$  isotope, while, at the same time, preferential dissolution of the heavier  $^{13}C$  isotope. Such kinetic fractionation during test dissolution cannot be readily explained. The extent to which microbial decomposition of organic matter within test chamber walls might cause such fractionation is also unconstrained. However, we find it unlikely that the observed isotope ratio offsets can be explained by this process.

The third and most likely process that can account for the observed isotopic offsets between well-preserved and altered tests is that alongside dissolution of specific domains within the bio-mineralized calcite in *Ci*-

POIRIER ET AL. 25 of 32



10.1029/2020PA004110

bicidoides specimens, inorganic calcite is precipitated (e.g., Detlef et al., 2020; Edgar et al., 2013; Sexton & Wilson, 2009; Sexton et al., 2006). Based on these results, we propose that (1) dissolution within internal domains of altered tests likely occurs shortly after the test is deposited but while still being influenced by the same water mass and (2) secondary diagenetic recrystallization also occurs within the upper sediment column. This inorganic calcite is likely sourced from aqueous carbonate species within porewaters, which migrate upward over time via sediment compaction. Therefore, the isotopic composition measured in altered tests reflects some combination of original material with that of interstitial porewaters. Ultimately, the isotopic composition of these porewaters could either reflect bottom waters at a given site from an older time period relative to the sampled interval (e.g., Schrag et al., 1996, 2002) or perhaps resemble the isotopic composition of carbonate materials being dissolved deeper within the sediment column.

Such a mechanism could explain why the stable isotopic composition in altered tests buried during the early deglaciation to middle Holocene interval reflects values more similar to glassy tests that were  $\sim$ 3–5 kyr older throughout the deglacial to middle Holocene interval, on average. A similar interpretation was made by Wycech et al. (2016) who found that during MIS 2 and the subsequent deglacial, radiocarbon measurements in opaque (frosty) planktic foraminifera tests produced older ages relative to translucent (glassy) planktic tests cooccurring in the same sediment horizons. Furthermore, reprecipitation of dissolved carbonate sourced from lower in the sediment column may also explain why the offsets in isotopic composition between well-preserved and altered tests reduce during the middle-to-late Holocene ( $\sim$ 6–0 ka),  $\sim$ 3–5 kyr after the  $\delta^{18}$ O and  $\delta^{13}$ C composition of seawater became relatively stable. Finally, our observation that tests from each preservation state are present in most assemblages, including those from many modern coretop samples (Plates S1–S53 in the Supporting Information), implies that significant alteration can begin very early following deposition (e.g., Edgar et al., 2013; Rudnicki et al., 2001).

#### 4.4.3. Robustness of Proxy Records Generated From Well-Preserved "Glassy" Tests

While the potential diagenetic biasing of proxy records is a major problem, especially when using geochemical analyses of pooled tests to reconstruct changes in the climate system, such as ice volume and sea level through time (Section 5), we would be remiss if we did not emphasize the quality of our stable isotope data from well-preserved glassy tests (Figure 11). The average  $\delta^{18}$ O and  $\delta^{13}$ C time series generated from glassy Cibicidoides specimens at Atlantic Site 929 produced records that show nearly perfect agreement with various other independent climate records (Figures 11a and 11b). For example, the deep-ocean temperature and global ice volume signals recorded in the glassy  $\delta^{18}$ O deglacial time series from Site 929 demonstrate millennial-scale variability that aligns with the NGRIP  $\delta^{18}$ O ice core record (Andersen et al., 2006; Rasmussen et al., 2006; Svensson et al., 2006, 2008; Vinther et al., 2006). This record documents changes in atmospheric temperature and ice volume in the Northern Hemisphere. Events that show comparable changes between these two records include the pronounced Bølling-Allerød warming event, the Younger Dryas cooling event, and smaller scale changes throughout the preindustrial Holocene (Figure 11a). Changes in the glassy  $\delta^{13}$ C deglacial time series from Site 929 correspond with changes in a water mass influence between the dominant northern-sourced NADW (more positive  $\delta^{13}$ C) versus southern-sourced AABW (more negative  $\delta^{13}$ C). The timing of the major changes in water mass influence at Site 929 agrees with the Pa/Th data set generated from the GGC5 sediment core recovered at similar depths on the Bermuda Rise (McManus et al., 2004), several thousand kilometers to the north (Figures 4 and 11b). Overall, these observations identify the continued and perhaps enhanced relevance of such records from the deep North Atlantic Ocean, when very carefully selecting only the best-preserved tests for analysis from every possible sample.

Our stable isotope time series from well-preserved glassy *Cibicidoides* specimens at Site 846 also demonstrate high-quality results from the deep Pacific Ocean during this deglacial interval (Figures 11c and 11d). The glassy  $\delta^{18}O$  record from Site 846 records changes in deep-ocean temperature and ice volume that coincide with similar changes in the composite  $CO_2$  ice core records from Antarctica (Bereiter et al., 2015), which was recently found to be nearly synchronous with changes in Antarctic temperature during this interval (Chowdhry Beeman et al., 2019). Comparable negative excursions in  $\delta^{18}O$  (i.e., deep-ocean warming and/or decreasing ice volume) and increases in  $CO_2$  (and temperature) over Antarctica in these records correspond with several distinct MP events beginning at  $\sim$ 17,  $\sim$ 15, and  $\sim$ 12 ka (Figure 11c). Finally, the positive excursions in the glassy  $\delta^{13}C$  record from Site 846, which records changes in water mass influence and in outgassing of isotopically light  $CO_2$  (i.e., of more negative  $\delta^{13}C$ ) to the atmosphere during this degla-

POIRIER ET AL. 26 of 32



10.1029/2020PA004110

cial interval, correspond with periods of increasing  $\Delta pCO_2$  in the surface ocean throughout the deglaciation at the nearby Site 1238 (Martínez-Botí et al., 2015) (Figures 4 and 11d). Overall, our stable isotope records generated from single glassy *Cibicidoides* tests from Sites 846 and Site 929 demonstrate the robustness of data that can be generated from the deep ocean when only well-preserved tests are analyzed.

#### 5. Conclusions and Implications

Through introducing the FPI, we defined visual criteria for identifying three preservation states of individual Cibicidoides and Uvigerina specimens (Section 2.1). Following these criteria, we further identified the domains within the chamber wall that are most affected by diagenesis, where visible "whitening" results from dissolution and subsequent inorganic calcite recrystallization (Section 2.2). By assessing the preservation quality of each test in a given sample, assemblage preservation can be quantified by applying the FPI scoring system (Section 3.3). Overall, we identify water mass chemistry, specifically water mass corrosivity, as the predominant influence on preservation quality (Sections 4.1 and 4.2). The FPI data demonstrate that as water mass corrosivity changes at a given site over glacial-interglacial cycles, corresponding regional and temporal changes in diagenesis also occur (Section 4.3). Our deglacial single-test stable isotope time series demonstrates that diagenesis can bias the geochemical composition of altered tests, likely through interactions with dissolved carbonate species in pore fluids advected upward through the sediment column, resulting in inorganic calcite recrystallization (Section 4.4). Ultimately, these results suggest that the majority of diagenetic alteration affecting these two benthic taxa occurs shortly after deposition, within the upper sediment column. While beyond the scope of this paper, additional diagenetic alteration may contribute to ongoing geochemical biasing in altered tests over longer time scales (e.g., Raymo et al., 2018; Sexton & Wilson, 2009). Overall, the findings from this work have major implications for the generation of proxy records, both those previously published and those to be generated in the future.

Most published geochemical proxy records generated from *Cibicidoides* and *Uvigerina* specimens are typically pooled, where 3–10 tests are analyzed for each individual data point. Of all the *Cibicidoides* (n=441) and *Uvigerina* assemblages (n=264) studied here, only 43.7% and 41.7% contained at least three ideally preserved glassy tests, respectively; with only 10.0% and 19.3% of *Cibicidoides* and *Uvigerina* assemblages containing at least 10 glassy tests, respectively (Table 2). The proportions of *Cibicidoides* and *Uvigerina* assemblages with at least 3 and 10 ideally preserved glassy tests varied by site (Table 2). As discussed above, the proportions of glassy tests in these assemblages are primarily influenced by the chemical composition and thereby the corrosivity of the deepwater mass at each site over orbital/glacial time scales.

Overall, the FPI assemblage preservation results alongside the observation of low percentages of assemblages at any given site containing  $\geq 3-10$  glassy tests ideal for geochemical analyses imply that published geochemical records produced from analyses of pooled *Cibicidoides* or *Uvigerina* specimens should be considered with an additional degree of uncertainty. The highest degree of additional uncertainty would be for data generated from interglacial samples recovered at sites in the deep Pacific and South Atlantic Oceans, as well as for data generated from glacial samples recovered from sites in the deep North Atlantic Ocean. Based on our observations, these intervals likely contain a relatively low proportion of well-preserved glassy tests, devoid of domains exhibiting significant dissolution (i.e., Figures 2 and 3) and/or recrystallization (i.e., Figures 9 and 10; Section 4.4), and are best identified by low FPI assemblage preservation scores (Figures 5-7). Furthermore, geochemical results from pooled analyses using benthic tests are likely biased to some degree.

Based on our single-test stable isotope records spanning the last deglaciation, the bias inherently present in proxy records likely varies through time (i.e., Figure 10). The inclusion of any altered tests in geochemical analyses is likely to have the most significant biasing effect during and immediately following periods of rapid change. For example, we found significant isotopic biasing within altered tests resulting in higher and lower  $\delta^{18}O$  and  $\delta^{13}C$  values, respectively, during the interval spanning the last deglaciation to middle Holocene (i.e., Figures 9 and 10). In both stable isotope records, altered tests generated isotopic values corresponding with those measured in glassy tests from samples that were at least  $\sim 3-5$  kyr older (Figure 9). This was particularly pronounced in samples representing the early-to-middle Holocene. This implies a high potential for the geochemical biasing of proxy records during the first  $\sim 5$  kyr of interglacial periods if

POIRIER ET AL. 27 of 32

10.1029/2020PA004110

one or several altered tests were included in pooled analyses. Such results are of particular significance to records used to reconstruct ice volume and sea level during past peak interglacial periods.

To provide estimates for the extent to which diagenetic bias might specifically affect sea-level reconstructions during early interglacial periods, we offer two simple mass balance scenarios. In this exercise, we consider 180 hypothetical benthic  $\delta^{18}$ O records generated from sites distributed throughout the global deep ocean, which have been combined into a stacked record (i.e., similar to that of Ahn et al. [2017]). Within these two scenarios, all of the individual benthic  $\delta^{18}$ O records were generated from pooled analyses of three *Cibicidoides* specimens, each of comparable mass. The first scenario considers biased records being generated by analyzing two glassy tests and one pseudo-glassy test per analysis. Comparatively, the second scenario considers biased records being generated by analyzing two glassy tests and one frosty test per analysis.

To estimate hypothetical diagenetic biasing in these two scenarios for the first ~5 kyr of an interglacial period, we consider the average  $\Delta\delta^{18}$ O offsets documented between glassy and pseudo-glassy tests (Site 929: 0.381%; Site 846: 0.095%) and between glassy and frosty tests (Site 929: 0.764%; Site 846: 0.178%) during the early-to-middle Holocene (Figure 10). Based on the observations noted herein, we propose that these two sites represent end-members of potential isotopic biasing due to diagenesis, while recognizing that there are likely sites exhibiting both lower and higher degrees of such bias. Therefore, to provide a more conservative estimate of potential bias within our hypothetical stacked benthic  $\delta^{18}$ O record, we assume one third of these hypothetical benthic  $\delta^{18}$ O records include no degree of diagenetic bias (i.e., represent the true climate signal, n = 60), one third exhibiting slight diagenetic bias (i.e., containing offsets similar to those documented at Site 846, n = 60), and one third being affected more substantially by diagenetic bias (i.e., containing offsets similar to those documented at Site 929, n = 60).

Following the conservative mass balance described above, our first scenario including one pseudo-glassy test per biased pooled analysis results in a hypothetical stacked  $\delta^{18}O$  record with an early interglacial value 0.159% heavier than the true value. Correspondingly, our second scenario including one frosty test per biased pooled analysis results in a hypothetical stacked  $\delta^{18}O$  record with an early interglacial value 0.314% heavier than the true signal. While these are hypothetical scenarios, such values strongly imply a large degree of diagenetic bias present in benthic proxy records used to reconstruct ice volume and therefore sea level, particularly during the first  $\sim$ 5 kyr of interglacial periods.

A global benthic  $\delta^{18}$ O change of 0.080%–0.110% represents approximately 10 m of sea-level equivalent ice volume change, when accounting for the temperature component influencing the  $\delta^{18}$ O<sub>sw</sub> (e.g., Adkins et al., 2002; Elderfield et al., 2012; Fairbanks, 1989; Fairbanks & Matthews, 1978; Raymo et al., 2018; Rohling et al., 2014; Schrag et al., 1996). While the hypothetical scenarios provided here imply a strong possibility for the misinterpretation of early interglacial sea-level estimates, we recognize that the true diagenetic bias present in any given published benthic  $\delta^{18}$ O record or in stacked benthic  $\delta^{18}$ O records such as those of Lisiecki and Raymo (2005) and Ahn et al. (2017) may be much lower. However, our documentation of the number of assemblages per site that contains at least three glassy *Cibicidoides* specimens (43.7% on average—Table 2) demonstrates the likelihood of diagenetic bias affecting any given records to some extent, and this exercise demonstrates that the effect of such biasing could be significant.

Despite our single-test stable isotope data spanning only the last deglaciation, our results imply that this biasing effect is likely pronounced during any period of rapid change, including during major stadial and interstadial events, as well as periods of glacial inception. The net result would be a delay in the true climatic signal, which for relatively short-lived events might significantly smooth, or even erase the amplitude of such an event within proxy reconstructions. Importantly, these findings also demonstrate that careful selection of benthic foraminifera recovered from deep-sea sediments for geochemical analyses can still generate very high-quality proxy reconstructions, even at millennial time scales (i.e., Figure 11). While the insights from our stable isotope data have particular significance to ice volume (i.e., sea level) and deep-ocean circulation records produced through stable isotope analyses, similar biasing likely affects other geochemical proxy reconstructions, future work should attempt to constrain additional degrees of uncertainty when interpreting published geochemical records, including stacked compilations of stable isotope records (i.e., Ahn et al., 2017; Imbrie et al., 1984; Lisiecki, 2014; Lisiecki & Raymo, 2005), as well

POIRIER ET AL. 28 of 32



Acknowledgments

We would like to thank the Interna-

tional Ocean Discovery Program as the

source of all core samples analyzed in

this study, as well as the U.S. Science

Support Program for funding two sum-

Ashley Braunthal and Claire Jasper for

help washing and processing sediment

samples. This work was primarily

funded by the NSF-OCE 1658230

research grant, with additional grant

Center at the Lamont-Doherty Earth

Observatory of Columbia University.

Additionally, the completion of this

U.S. Geological Survey Land Change

Program. We would like to thank Dr

Thomas M. Cronin and Dr Marci M.

reviews of this manuscript including

comments and suggestions, as well as

al anonymous reviewer for considera-

tion of the publication of this work in

names is for descriptive purposes only

and does not imply endorsement by the

Any use of trade, firm, or product

U.S. Government.

Paleoceanography and Paleoclimatology.

those of Dr Phil Sexton and an addition-

Robinson for their useful USGS internal

manuscript was partially funded by the

funding for the single-test stable isotope

analyses being provided by The Climate

mer REU fellowships. Thanks also to

# Paleoceanography and Paleoclimatology

10.1029/2020PA004110

as the degree of inherent bias in other geochemical records. To aid in the selection of well-preserved glassy tests for geochemical analyses in future studies, we include images of tests representing each preservation state (Plates S1–S6 in the Supporting Information), as well as all *Cibicidoides* specimens from which we generated the single-test stable isotope data illustrated in Figures 9 and 10 (Plates S7–S53 in the Supporting Information). Ultimately, these plates demonstrate the range of preservation quality within pseudo-glassy tests, which may look relatively well preserved but can substantially alter geochemical results in pooled analyses, and along with more easily recognized frosty tests should be avoided.

#### **Data Availability Statement**

Detailed data tables of single-test  $\delta^{18}O$  and  $\delta^{13}C$  analyses, test mass, sample ages, and preservation scores are available in the Supporting Information and from the PANGAEA Data Publisher (https://doi.pangaea. de/10.1594/PANGAEA.924695, https://doi.pangaea.de/10.1594/PANGAEA.924671, https://doi.pangaea.de/10.1594/PANGAEA.924673, and https://doi.pangaea.de/10.1594/PANGAEA.924743).

#### References

Adkins, J. F., McIntyre, K., & Schrag, D. P. (2002). The salinity, temperature, and δ<sup>18</sup>O of the glacial deep ocean. *Science*, 298, 1769–1773. Ahn, S., Khider, D., Lisiecki, L. E., & Lawrence, C. E. (2017). A probabilistic Pliocene–Pleistocene stack of benthic δ<sup>18</sup>O using a profile hidden Markov model. *Dynamics and Statistics of the Climate System*, 2(1). https://doi.org/10.1093/climsys/dzx002

Allen, K. A., Sikes, E. L., Hönisch, B., Elmore, A. C., Guilderson, T. P., Rosenthal, Y., & Anderson, R. F. (2015). Southwest Pacific deep water carbonate chemistry linked to high southern latitude climate and atmospheric CO<sub>2</sub> during the Last Glacial Termination. *Quaternary Science Reviews*, 122, 180–191.

Andersen, K. K., Svensson, A., Johnsen, S. J., Rasmussen, S. O., Bigler, M., Rothlisberger, R., et al. (2006). The Greenland ice core chronology 2005, 15–42 ka. Part 1: Constructing the time scale. *Quaternary Science Reviews*, 25(23–24), 3246–3257.

Barker, S., Diz, P., Vautravers, M. J., Pike, J., Knorr, G., Hall, I. R., & Broecker, W. S. (2009). Interhemispheric Atlantic seesaw response during the last deglaciation. *Nature*, 457, 1097–1102.

Barker, S., Knorr, G., Vautravers, M. J., Diz, P., & Skinner, L. C. (2010). Extreme deepening of the Atlantic overturning circulation during deglaciation. *Nature Geoscience*, 3, 567–571.

Bereiter, B., Eggleston, S., Schmitt, J., Nehrbass-Ahles, C., Stocker, T. F., Fischer, H., et al. (2015). Revision of the EPICA Dome C CO<sub>2</sub> record from 800 to 600 kyr before present. *Geophysical Research Letters*, 42, 542–549. https://doi.org/10.1002/2014GL061957

Bickert, T., Curry, W. B., & Wefer, G. (1997). Late Pliocene to Holocene (2.6–0 Ma) western equatorial Atlantic deep-water circulation: Inferences from benthic stable isotope records. In N. J. Shackleton, W. B. Curry, C. Richter, & T. J. Bralower (Eds.), Proceedings of the Ocean Drilling Program, Scientific Results (Vol. 154). College Station, TX: Ocean Drilling Program. https://doi.org/10.2973/opd.proc. ir.154.1997

Billups, K., Ravelo, A. C., & Zachos, J. C. (1998). Early Pliocene deep water circulation in the western equatorial Atlantic: Implications for high-latitude climate change. *Paleoceanography*, 13(1), 84–95.

Billups, K., & Schrag, D. P. (2002). Paleotemperatures and ice volume of the past 27 Myr revisited with paired Mg/Ca and <sup>18</sup>O/<sup>16</sup>O measurements on benthic foraminifera. *Paleoceanography*, 17(1), 1003. https://doi.org/10.1029/2000PA000567

Böhm, E., Lippold, J., Gutjahr, M., Frank, M., Blaser, P., Antz, B., et al. (2015). Strong and deep Atlantic meridional overturning circulation during the last glacial cycle. *Nature*, 517, 73–76.

Bostock, H. C., Hayward, B. W., Neil, H. L., Currie, K. I., & Dunbar, G. B. (2011). Deep-water carbonate concentrations in the southwest Pacific. Deep Sea Research Part I: Oceanographic Research Papers, 58, 72–85.

Bostock, H. C., Mikaloff Fletcher, S. E., & Williams, M. J. M. (2013). Estimating carbonate parameters from hydrographic data for the intermediate and deep waters of the Southern Hemisphere oceans. *Biogeosciences*, 10, 6199–6213.

Bralower, T. J., Premoli Sivla, I., & Malone, M. J., (2002). Proceedings of the Ocean Drilling Program, Initial Reports (Vol. 198). College Station, TX: Ocean Drilling Program. https://doi.org/10.2973/opd.proc.ir.198.2002

Broecker, W. S. (2006). The oceanic CaCO<sub>3</sub> cycle. In H. Edlerfield, H. D. Holland, H. Elderfield, & K. K. Turekian (Eds.), The oceans and marine geochemistry (Vol. 6, pp. 529–549). Amsterdam, The Netherlands: Elsevier.

Burke, A., & Robinson, L. F. (2012). The Southern Ocean's role in carbon exchange during the last deglaciation. Science, 335, 557-561.

Cheng, X., Tian, J., & Wang, P. (2004). Data report: Stable isotopes from Site 1143. In W. L. Prell, P. Wang, P. Blum, D. K. Rea, & S. C. Clemens (Eds.), Proceedings of the Ocean Drilling Program, Scientific Results (Vol. 184). College Station, TX: Ocean Drilling Program. https://doi.org/10.2973/opd.proc.ir.184.2004

Chen, T., Robinson, L. F., Burke, A., Southon, J., Spooner, P., Morris, P. J., & Ng, H. C. (2015). Synchronous centennial abrupt events in the ocean and atmosphere during the last deglaciation. *Science*, 349(6255), 1537–1541.

Chowdhry Beeman, J., Gest, L., Parrenin, F., Raynaud, D., Fudge, T. J., Buizert, C., & Brook, E. J. (2019). Antarctic temperature and CO<sub>2</sub>: Near-synchrony yet variable phasing during the last deglaciation. *Climate of the Past*, 15, 913–926.

Clark, P. U., Shakun, J. D., Baker, P. A., Bartlein, P. J., Brewer, S., Brook, E., et al. (2012). Global climate evolution during the last deglaciation. *Proceedings of the National Academy of Sciences*, 109(19), E1134–E1142.

Curry, W. B., Shackleton, N. J., Richter, C., Backman, J. E., Bassinot, F., Bickert, T., et al. (1995). *Proceedings of the Ocean Drilling Program, Initial Reports* (Vol. 154). College Station, TX: Ocean Drilling Program. <a href="https://doi.org/10.2973/opd.proc.ir.154.1995">https://doi.org/10.2973/opd.proc.ir.154.1995</a>

deMenocal, P., Archer, D., & Leth, P. (1997). Pleistocene variations in deep Atlantic circulation and calcite burial between 1.2 and 0.6 Ma: A combined data-model approach. In N. J. Shackleton, W. B. Curry, C. Richter, & T. J. Bralower (Eds.), Proceedings of the Ocean Drilling Program, Scientific Results (Vol. 154). College Station, TX: Ocean Drilling Program. https://doi.org/10.2973/opd.proc.ir.154.1997

Detlef, H., Sosdian, S. M., Kender, S., Lear, C. H., & Hall, I. R. (2020). Multi-elemental composition of authigenic carbonates in benthic foraminifera from the eastern Bering Sea continental margin (International Ocean Discovery Program Site U1343). *Geochimica et Cosmochimica Acta*, 268, 1–21.

POIRIER ET AL. 29 of 32



10.1029/2020PA004110

- Dowsett, H. J., Robinson, M. M., & Foley, K. M. (2009). Pliocene three-dimensional global ocean temperature reconstruction. *Climate of the Past*. 5, 769–783.
- Dowsett, H. J., Robinson, M. M., Foley, K. M., Herbert, T. D., Otto-Bliesner, B. L., & Spivey, W. (2019). The mid-Piacenzian of the North Atlantic Ocean. *Stratigraphy*, 16(3), 119–144.
- Du, J., Haley, B. A., Mix, A. C., Walczak, M. H., & Praetorius, S. K. (2018). Flushing of the deep Pacific Ocean and the deglacial rise of atmospheric CO<sub>2</sub> concentrations. *Nature Geoscience*, 11, 749–755.
- Gupta, B. K. S. (Ed.). (1999). Modern foraminifera. Amsterdam, The Netherlands: Springer-Science+Business Media, B.V. https://doi.org/10.1007/978-0-306-48104-8
- Edgar, K. M., Pälike, H., & Wilson, P. A. (2013). Testing the impact of diagenesis on the  $\delta^{18}O$  and  $\delta^{13}C$  of benthic foraminiferal calcite from a sediment burial depth transect in the equatorial Pacific. *Paleoceanography*, 28, 468–480. https://doi.org/10.1002/palo.20045
- Elderfield, H., Ferretti, P., Greaves, M., Crowhurst, S., McCave, I. N., Hodell, D., & Piotrowski, A. M. (2012). Evolution of ocean temperature and ice volume through the mid-Pleistocene climate transition. *Science*, 337, 704–709.
- Elderfield, H., Greaves, M., Barker, S., Hall, I. R., Tripati, A., Ferretti, P., et al. (2010). A record of bottom water temperature and seawater δ<sup>18</sup>O for the Southern Ocean over the past 440 kyr based on Mg/Ca of benthic foraminiferal *Uvigerina* spp. *Quaternary Science Reviews*, 29, 160–169.
- Emiliani, C. (1955). Pleistocene temperatures. The Journal of Geology, 63(6), 538-578.
- Ezat, M. M., Rasmussen, T. L., Thornalley, D. J. R., Olsen, J., Skinner, L. C., Hönisch, B., & Groeneveld, J. (2017). Ventilation history of Nordic Seas overflows during the last (de)glacial period revealed by species-specific benthic foraminiferal <sup>14</sup>C dates. *Paleoceanography*, 32, 172–181. https://doi.org/10.1002/2016PA003053
- Fairbanks, R. G. (1989). A 17,000-year glacio-eustatic sea level record: Influence of glacial melting rates on the Younger Dryas event and deep-ocean circulation. *Nature*, 342, 637–642.
- Fairbanks, R. G., & Matthews, R. K. (1978). The marine oxygen isotope record in Pleistocene coral, Barbados, West Indies. Quaternary Research, 10, 181–196.
- Fantle, M. S., Maher, K. M., & DePaolo, D. J. (2010). Isotopic approaches for quantifying the rates of marine burial diagenesis. *Reviews of Geophysics*, 48, RG3002. https://doi.org/10.1029/2009RG000306
- Ford, H. L., Sosdian, S. M., Rosenthal, Y., & Raymo, M. E. (2016). Gradual and abrupt changes during the mid-Pleistocene transition. Ouaternary Science Reviews. 148. 222–233.
- Franz, S. O., & Tiedemann, R. (2002). Depositional changes along the Blake-Bahama Outer Ridge deep water transect during marine isotope stages 8 to 10—Links to the Deep Western Boundary Current. *Marine Geology*, 189, 107–122.
- Gebbie, G. (2014). How much did Glacial North Atlantic Water shoal? *Paleoceanography*, 29, 190–209. https://doi.org/10.1002/2013PA002557 Gersonde, R., Hodell, D. A., Blum, P., Andersson, C., Austin, W. E. N., Billups, K., et al. (1999). *Proceedings of the Ocean Drilling Program*,
- Initial Reports (Vol. 177). College Station, TX: Ocean Drilling Program, https://doi.org/10.2973/opd.proc.ir.177.1999
  Gottschalk, J., Vázquez Riveiros, N., Waelbroeck, C., Skinner, L. C., Michel, E., Duplessy, J.-C., et al. (2016). Carbon isotope offsets between
- Gottschalk, J., Vázquez Riveiros, N., Waelbroeck, C., Skinner, L. C., Michel, E., Duplessy, J.-C., et al. (2016). Carbon isotope offsets between benthic foraminifer species of the genus *Cibicides* (*Cibicidoides*) in the glacial sub-Antarctic Atlantic. *Paleoceanography*, 31, 1583–1602. https://doi.org/10.1002/2016PA003029
- Grützner, J., Giosan, L., Franz, S. O., Tiedemann, R., Cortijo, E., Chaisson, W. P., et al. (2002). Astronomical age models for Pleistocene drift sediments from the western North Atlantic (ODP Sites 1055–1063). *Marine Geology*, 189, 5–23.
- Gray, W. R., Wills, R. C. J., Rae, J. W. B., Burke, A., Ivanovic, R. F., Roberts, W. H. G., et al. (2020). Wind-driven evolution of the North Pacific subpolar gyre over the last deglaciation. *Geophysical Research Letters*, 47, e2019GL086328. https://doi.org/10.1029/2019GL086328
- Hagen, S., & Keigwin, L. D. (2002). Sea-surface temperature variability and deep water reorganisation in the subtropical North Atlantic during Isotope Stage 2–4. *Marine Geology*, 189, 145–162.
- Harris, S. E., Mix, A. C., & King, T. (1997). Biogenic and terrigenous sedimentation at Ceara Rise, western tropical Atlantic, Supports Pliocene–Pleistocene deep-water linkage between hemispheres. In N. J. Shackleton, W. B. Curry, C. Richter, & T. J. Bralower (Eds.), Proceedings of the Ocean Drilling Program, Scientific Results (Vol. 154, pp. 331–345). College Station, TX: Ocean Drilling Program.
- Hasenfratz, A. P., Martínez-García, A., Jaccard, S. L., Vance, D., Wälle, M., Greaves, M., & Haug, G. H. (2017). Determination of the Mg/Mn ratio in foraminiferal coatings: An approach to correct Mg/Ca temperatures for Mn-rich contaminant phases. *Earth and Planetary Science Letters*, 457, 335–347.
- Herguera, J. C., Herbert, T., Kashgarian, M., & Charles, C. (2010). Intermediate and deep water mass distribution in the Pacific during the Last Glacial Maximum inferred from oxygen and carbon stable isotopes. *Quaternary Science Reviews*, 29, 1228–1245.
- Herguera, J. C., Jansen, E., & Berger, W. H. (1992). Evidence for a bathyal front at 2000-M depth in the glacial Pacific, based on a depth transect on Ontong Java Plateau. *Paleoceanography*. 7(3), 273–288.
- Hess, S., & Kuhnt, W. (2005). Neogene and Quaternary paleoceanographic changes in the southern South China Sea (Site 1143): The benthic foraminiferal record. *Marine Micropaleontology*, 54(1–2), 63–87.
- Hodell, D. A., Charles, C. D., Curtis, J. H., Mortyn, P. G., Ninnemann, U. S., & Venz, K. A. (2003). 9. Data report: Oxygen isotope stratigraphy of ODP Leg 177 Sites 1088, 1089, 1090, 1093, and 1094. In R. Gersonde, D. A. Hodell, & P. Blum (Eds.), Proceedings of the Ocean Drilling Program, Scientific Results (Vol. 177). College Station, TX: Ocean Drilling Program. https://doi.org/10.2973/odp.proc.sr.177.2003
- Hodell, D. A., Charles, C. D., & Sierro, F. J. (2001). Late Pleistocene evolution of the ocean's carbonate system. *Earth and Planetary Science Letters*, 192, 109–124.
- Howe, J. N. W., Piotrowski, A. M., Noble, T. L., Mulitza, S., Chiessi, C. M., & Bayon, G. (2016). North Atlantic Deep Water production during the Last Glacial Maximum. *Nature Communications*, 7(1), 1–8.
- Imbrie, J., Hays, J. D., Martinson, D. G., McIntyre, A., Mix, A. C., Morley, J. J., et al. (1984). The orbital theory of Pleistocene climate: Support from a revised chronology of the marine  $\delta^{18}$ O record. In A. L. Berger, et al. (Eds.), *Milankovich and climate, Part 1* (pp. 269–305). Dordrecht, Holland: D. Reidel Publishing Company.
- Jian, Z., Zhao, Q., Cheng, X., Wang, J., Wang, P., & Su, X. (2003). Pliocene-Pleistocene stable isotope and paleoceanographic changes in the northern South China Sea. Palaeogeography, Palaeoclimatology, Palaeoecology, 193, 425-442.
- Johnstone, H. J. H., Schulz, M., Barker, S., & Elderfield, H. (2010). Inside story: An X-ray computed tomography method for assessing dissolution in the tests of planktonic foraminifera. Marine Micropaleontology, 77, 58–70.
- Keigwin, L. D. (1998). Glacial-age hydrography of the far northwest Pacific Ocean. Paleoceanography, 13(4), 323-339.
- Keigwin, L. J., Rio, D., Acton, G. D., Bianchi, G. G., Borowski, W., Cagatay, N., et al. (1998). Proceedings of the Ocean Drilling Program, Initial Reports (Vol. 172). College Station, TX: Ocean Drilling Program. https://doi.org/10.2973/opd.proc.ir.172.1998
- Kwiek, P. B., & Ravelo, A. C. (1999). Pacific Ocean intermediate and deep water circulation during the Pliocene. Palaeogeography, Palaeoclimatology, Palaeoecology, 154, 191–217.

POIRIER ET AL. 30 of 32

- Lear, C. H., Elderfield, H., & Wilson, P. (2000). Cenozoic deep-sea temperatures and global ice volumes from Mg/Ca in benthic foraminiferal calcite. *Science*, 287(5451), 269–272.
- Leutert, T. J., Sexton, P. F., Tripati, A., Piasecki, A., Ho, S. L., & Meckler, A. N. (2019). Sensitivity of clumped isotope temperatures in fossil benthic and planktic foraminifera to diagenetic alteration. *Geochimica et Cosmochimica Acta*, 257, 354–372.
- Lisiecki, L. E. (2014). Atlantic overturning responses to obliquity and precession over the last 3 Myr. *Paleoceanography*, 29, 71–86. https://doi.org/10.1002/2013PA002505
- Lisiecki, L. E., & Raymo, M. E. (2005). A Pliocene–Pleistocene stack of 57 globally distributed benthic δ<sup>18</sup>O records. *Paleoceanography*, 20, PA1003. https://doi.org/10.1029/2004PA001071
- Lund, D. C., Tessin, A. C., Hoffman, J. L., & Schmittner, A. (2015). Southwest Atlantic water mass evolution during the last deglaciation. Paleoceanography, 30, 477–494. https://doi.org/10.1002/2014PA002657
- Mackensen, A., Hubberten, H.-W., Bickert, T., Fischer, G., & Fütterer, D. K. (1993). The  $\delta^{13}$ C in benthic foraminiferal tests of *Fontbotia wuellerstorfi* (Schwager) relative to the  $\delta^{13}$ C of dissolved inorganic carbon in Southern Ocean Deep Water: Implications for glacial ocean circulation models. *Paleoceanography*, 8(5), 587–610.
- Martínez-Botí, M. A., Marino, G., Foster, G. L., Ziveri, P., Henehan, M. J., Rae, J. W. B., et al. (2015). Boron isotope evidence for oceanic carbon dioxide leakage during the last deglaciation. *Nature*, 518(7538), 219–222.
- Matsumoto, K., Oba, T., Lynch-Stieglitz, J., & Yamamoto, H. (2002). Interior hydrography and circulation of the glacial Pacific Ocean. *Quaternary Science Reviews*, 21(14–15), 1693–1704.
- Mayer, L., Pisias, N., Janecek, T., Baldauf, J. G., Bloomer, S. F., Dadey, K. A., et al. (1992). Proceedings of the Ocean Drilling Program, Initial Reports (Vol. 138). College Station, TX: Ocean Drilling Program. https://doi.org/10.2973/opd.proc.ir.138.1992
- McCorkle, D. C., Martin, P. A., Lea, D. W., & Klinkhammer, G. P. (1995). Evidence of a dissolution effect on benthic foraminiferal shell chemistry: δ<sup>13</sup>C, Cd/Ca, Ba/Ca, and Sr/Ca results from the Ontong Java Plateau. *Paleoceanography*, 10(4), 699–714.
- McManus, J. F., Francois, R., Gherardi, J.-M., Keigwin, L. D., & Brown-Leger, S. (2004). Collapse and rapid resumption of Atlantic meridianal distribution linked to declarid dimeter changes. *Nature* 428, 824, 827
- onal circulation linked to deglacial climate changes. *Nature*, 428, 834–837. Millo, C., Sarnthein, M., Erlenkeuser, H., & Frederichs, T. (2005). Methane-driven late Pleistocene  $\delta^{13}$ C minima and overflow reversals in the southwestern Greenland Sea. *Geology*, 33(11), 873–876.
- Mix, A. C., Le, J., & Shackleton, N. J. (1995). Benthic foraminiferal stable isotope stratigraphy of Site 846: 0–1.8 Ma. In N. G. Pisias, L. A. Mayer, T. R. Janecek, A. Palmer-Julson, & T. H. van Andel (Eds.), Proceedings of the Ocean Drilling Program, Scientific Results (Vol. 138). College Station, TX: Ocean Drilling Program. https://doi.org/10.2973/opd.proc.ir.138.1995
- Mulitza, S., Chiessi, C. M., Schefuß, E., Lippold, J., Wichmann, D., Antz, B., et al. (2017). Synchronous and proportional deglacial changes in Atlantic meridional overturning and northeast Brazilian precipitation. *Paleoceanography*, 32, 622–633. https://doi.org/10.1002/2017PA003084
- Okazaki, Y., Timmermann, A., Menviel, L., Harada, N., Abe-Ouchi, A., Chikamoto, M. O., et al. (2010). Deepwater formation in the North Pacific during the last glacial termination. *Science*, 329(5988), 200–204.
- Olsen, A., Key, R. M., van Heuven, S., Lauvset, S. K., Velo, A., Lin, X., et al. (2016). The Global Ocean Data Analysis Project version 2 (GLODAPv2)—An internally consistent data product for the world ocean. *Earth System Science Data*, 8(2), 297–323.
- Oppo, D. W., Gebbie, G., Huang, K. F., Curry, W. B., Marchitto, T. M., & Pietro, K. R. (2018). Data constraints on glacial Atlantic water mass geometry and properties. *Paleoceanography and Paleoclimatology*, 33, 1013–1034. https://doi.org/10.1029/2018PA003408
- Pearson, P. N., & Burgess, C. E. (2008). Foraminifer test preservation and diagenesis: Comparison of high latitude Eocene sites. *Geological Society of London, Special Publications*, 303(1), 59–72.
- Poirier, R. K., & Billups, K. (2014). The intensification of northern component deepwater formation during the mid-Pleistocene climate transition. *Paleoceanography*, 29, 1046–1061. https://doi.org/10.1002/2014PA002661
- Rasmussen, S. O., Andersen, K. K., Svensson, A. M., Steffensen, J. P., Vinther, B. M., Clausen, H. B., et al. (2006). A new Greenland ice core chronology for the last glacial termination. *Journal of Geophysical Research*, 111, D06102. https://doi.org/10.1029/2005JD006079
- Raymo, M. E., Kozdon, R., Evans, D., Lisiecki, L., & Ford, H. L. (2018). The accuracy of mid-Pliocene δ<sup>18</sup>O-based ice volume and sea level reconstructions. *Earth-Science Reviews*, 177, 291–302.
- Raymo, M. E., Ruddiman, W. F., Backman, J., Clement, B. M., & Martinson, D. G. (1989). Late Pliocene variation in Northern Hemisphere ice sheets and North Atlantic deep water circulation. *Paleoceanography*, 4(4), 413–446.
- Rohling, E. J., Foster, G. L., Grant, K. M., Marino, G., Roberts, A. P., Tamisiea, M. E., & Williams, F. (2014). Sea-level and deep-sea-temper-ature variability over the past 5.3 million years. *Nature*, 508(7497), 477–482.
- Ronge, T. A., Tiedemann, R., Lamy, F., Köhler, P., Alloway, B. V., De Pol-Holz, R., et al. (2016). Radiocarbon constraints on the extent and evolution of the South Pacific glacial carbon pool. *Nature Communications*, 7, 11487.
- Rosenthal, Y., Boyle, E. A., & Slowey, N. (1997). Temperature control on the incorporation of magnesium, strontium, fluorine, and cadmium into benthic foraminiferal shells from Little Bahama Bank: Prospects for thermocline paleoceanography. *Geochimica et Cosmochimica Acta*, 61(17), 3633–3643.
- Ruddiman, W. F., Raymo, M. E., Martinson, D. G., Clement, B. M., & Backman, J. (1989). Pleistocene evolution: Northern hemisphere ice sheets and North Atlantic Ocean. *Paleoceanography*, 4(4), 353–412.
- Rudnicki, M. D., Wilson, P. A., & Anderson, W. T. (2001). Numerical models of diagenesis, sediment properties, and pore fluid chemistry on a paleoceanographic transect: Blake Nose, Ocean Drilling Program Leg 171B. *Paleoceanography*, 16(6), 563–575.
- Schlitzer, R. (2020). Ocean Data View. Retrieved from https://odv.awi.de
- Schrag, D. P., Adkins, J. F., McIntyre, K., Alexander, J. L., Hodell, D. A., Charles, C. D., & McManus, J. F. (2002). The oxygen isotopic composition of seawater during the Last Glacial Maximum. *Quaternary Science Reviews*, 21, 331–342.
- Schrag, D. P., Hampt, G., & Murray, D. W. (1996). Pore fluid constraints on the temperature and oxygen isotopic composition of the glacial ocean. *Science*, 272, 1930–1932.
- Sexton, P. F., & Barker, S. (2012). Onset of 'Pacific-style' deep-sea sedimentary carbonate cycles at the mid-Pleistocene transition. *Earth and Planetary Science Letters*, 321–322, 81–94.
- Sexton, P. F., & Wilson, P. A. (2009). Preservation of benthic foraminifera and reliability of deep-sea temperature records: Importance of sedimentation rates, lithology, and the need to examine test wall structure. *Paleoceanography*, 24, PA2208. https://doi.org/10.1029/2008PA001650
- Sexton, P. F., Wilson, P. A., & Pearson, P. N. (2006). Microstructural and geochemical perspectives on planktic foraminiferal preservation: "Glassy" versus "Frosty". Geochemistry, Geophysics, Geosystems, 7, Q12P19. https://doi.org/10.1029/2006GC001291
- Shackleton, N. (1967). Oxygen isotope analyses and Pleistocene temperatures re-assessed. Nature, 215(5096), 15-17.

POIRIER ET AL. 31 of 32



10.1029/2020PA004110

- Shackleton, N. J., & Hall, M. A. (1984). Carbon isotope data from Leg 74 sediments. In *Deep Sea Drilling Project Reports and Publications*. https://doi.org/10.2973/dsdp.proc.74.116.1984
- Shackleton, N. J., Hall, M. A., & Boersma, A. (1984). Oxygen and carbon isotope data from Leg 74 foraminifers. In *Deep Sea Drilling Project Reports and Publications*. https://doi.org/10.2973/dsdp.proc.74.115.1984
- Shackleton, N. J., Hall, M. A., & Pate, D. (1995). Pliocene stable isotope stratigraphy of Site 846. In N. G. Pisias, L. A. Mayer, T. R. Janecek, A. Palmer-Julson, & T. H. van Andel (Eds.), Proceedings of the Ocean Drilling Program, Scientific Results (Vol. 138). College Station, TX: Ocean Drilling Program. https://doi.org/10.2973/opd.proc.ir.138.1995
- Sikes, E. L., Allen, K. A., & Lund, D. C. (2017). Enhanced  $\delta^{13}C$  and  $\delta^{18}O$  differences between the South Atlantic and South Pacific during the last glaciation: The deep gateway hypothesis. *Paleoceanography*, 32, 1000–1017. https://doi.org/10.1002/2017PA003118
- Sikes, E. L., Elmore, A. C., Allen, K. A., Cook, M. S., & Guilderson, T. P. (2016). Glacial water mass structure and rapid δ<sup>18</sup>O and δ<sup>13</sup>C changes during the last glacial termination in the Southwest Pacific. *Earth and Planetary Science Letters*, 456, 87–97.
- Skinner, L., McCave, I. N., Carter, L., Fallon, S., Scrivner, A. E., & Primeau, F. (2015). Reduced ventilation and enhanced magnitude of the deep Pacific carbon pool during the last glacial period. *Earth and Planetary Science Letters*, 411, 45–52.
- Sosdian, S. M., Rosenthal, Y., & Toggweiler, J. R. (2018). Deep Atlantic carbonate ion and CaCO<sub>3</sub> compensation during the Ice Ages. *Paleoceanography and Paleoclimatology*, 33, 546–562. https://doi.org/10.1029/2017PA003312
- Sosdian, S., & Rosenthal, Y. (2009). Deep-sea temperature and ice volume changes across the Pliocene–Pleistocene climate transitions. Science, 325(5938), 306–310.
- Svensson, A., Andersen, K. K., Bigler, M., Clausen, H. B., Dahl-Jensen, D., Davies, S. M., et al. (2006). The Greenland ice core chronology 2005, 15–42 ka. Part 2: Comparison to other records. *Quaternary Science Reviews*, 25(23–24), 3258–3267.
- Svensson, A., Andersen, K. K., Bigler, M., Clausen, H. B., Dahl-Jensen, D., Davies, S. M., et al. (2008). A 60 000 year Greenland stratigraphic ice core chronology. Climate of the Past, 4(1), 47–57.
- Troupin, C., Barth, A., Sirjacobs, D., Ouberdous, M., Brankart, J.-M., Brasseur, P., et al. (2012). Generation of analysis and consistent error fields using the Data Interpolating Variational Analysis (DIVA). *Ocean Modelling*, 52–53, 90–101.
- Ullermann, J., Lamy, F., Ninnemann, U., Lembke-Jene, L., Gersonde, R., & Tiedemann, R. (2016). Pacific–Atlantic Circumpolar Deep Water coupling during the last 500 ka. *Paleoceanography*, 31, 639–650. https://doi.org/10.1002/2016PA002932
- Venti, N. L., & Billups, K. (2012). Stable-isotope stratigraphy of the Pliocene–Pleistocene climate transition in the northwestern subtropical Pacific. *Palaeogeography, Palaeoclimatology, Palaeoccology*, 326–328, 54–65.
- Vinther, B. M., Clausen, H. B., Johnsen, S. J., Rasmussen, S. O., Andersen, K. K., Buchardt, S. L., et al. (2006). A synchronized dating of three Greenland ice cores throughout the Holocene. *Journal of Geophysical Research*, 111, D13102. https://doi.org/10.1029/2005JD006921
- Waelbroeck, C., Labeyrie, L., Michel, E., Duplessy, J. C., McManus, J. F., Lambeck, K., et al. (2002). Sea-level and deep water temperature changes derived from benthic foraminifera isotopic records. *Quaternary Science Reviews*, 21, 295–305.
- Wang, P., Prell, W. L., Blum, P., Arnold, E. M., Bühring, C. J., Chen, M.-P., et al. (2000). Proceedings of the Ocean Drilling Program, Initial Reports (Vol. 184). College Station, TX: Ocean Drilling Program. https://doi.org/10.2973/opd.proc.ir.184.2000
- Wilkens, R. H., Westerhold, T., Drury, A. J., Lyle, M., Gorgas, T., & Tian, J. (2017). Revisiting the Ceara Rise, equatorial Atlantic Ocean: Isotope stratigraphy of ODP Leg 154 from 0 to 5 Ma. Climate of the Past, 13, 779–793.
- Wycech, J., Kelly, D. C., & Marcott, S. (2016). Effects of seafloor diagenesis on planktic foraminiferal radiocarbon ages. *Geology*, 44(7),
- Zarriess, M., & Mackensen, A. (2011). Testing the impact of seasonal phytodetritus deposition on δ<sup>13</sup>C of epibenthic foraminifer Cibicidoides wuellerstorfi: A 31,000 year high-resolution record from the northwest African continental slope. Paleoceanography, 26, PA2202. https://doi.org/10.1029/2010PA001944
- Zhang, J., Liu, Z., Brady, E. C., Oppo, D. W., Clark, P. U., Jahn, A., et al. (2017). Asynchronous warming and δ<sup>18</sup>O evolution of deep Atlantic water masses during the last deglaciation. *Proceedings of the National Academy of Sciences of the United States of America*, 114(42), 11075–11080.

POIRIER ET AL. 32 of 32